MINISTRY OF EDUCATION AND TRAINING
HO CHI MINH CITY UNIVERSITY OF
TECHNOLOGY AND EDUCATION

VO LAM CHUONG

STUDY ON MODELING AND FRACTIONAL-ORDER CONTROL FOR MULTIVARIABLE PROCESSES

ABSTRACT OF DISSERTATION

MAJOR: MECHANICAL ENGINEERING
CODE: 9520103

Ho Chi Minh City, 06/2024

CURRICULUM VITAE

I. INFORMATION

Name: VO LAM CHUONG　　　　Sex: Male

Born: 19/11/1979　　　　Birthplace: Khanh Hoa

II. TRAINING

1997 – 2002: Student at Technical University, Ho Chi Minh City, Faculty: Electrical-Electronics Engineering

2002 – 2005: Undergraduate student (Master) at Technical University, Ho Chi Minh City, Major: Cybernetics

2016 – now: PhD candidate at Ho Chi Minh City University of Technology and Education, Major: Mechanical Engineering

III. WORKING

2005 – now: Lecturer of Mechatronics Department, Mechanical Engineering Faculty, Ho Chi Minh City University of Technology and Education.

Tp.HCM, day month year 2024

Vo Lam Chuong

DECLARATION OF AUTHORSHIP

I hereby declare that this thesis was carried out by myself under the guidance and supervision of a team of scientists and cited references. The research results presented in the thesis are honest, objective and have never been published in any other work.

Tp.HCM, day month year 2024

Author

Vo Lam Chuong

ACKNOWLEDGMENT

First of all, I would like to sincerely thank Assoc. Prof. Truong Nguyen Luan Vu for his valuable guidance and suggestions throughout the thesis. I would also like to thank the group of professors at Yeungnam University, Korea, Prof. Lee, Prof. Nguyen, and Prof. Jae Hak Jung, who helped me in the publication of the articles.

I would like to send special thanks to the Faculty of Mechanical Engineering and other faculties and offices along with many friends and colleagues of the HCM City University of Technology and Education, who has helped and supported me throughout the study and research.

I would like to express my sincere thanks to the professors of all seminars for their valuable time and advice.

Finally, I would like to thank my family, especially my wife, for their support, help, and sharing in life difficulties. My family has always been my strong support throughout the thesis research.

Sincerely,

Vo Lam Chuong

CONTENTS

Curriculum Vitae i
Declaration authorship i
Acknowledgment ii
Symbols and abbreviations v
List of figures vii
List of tables ix
Abstract x
Tóm tắt xi
INTRODUCTION **1**
1. Problem statement 1
2. Research goals 1
3. Research scopes 1
4. Research approach and methods 1
5. Scientific and practical contributions 1
6. Thesis structure 2
Chapter 1. OVERVIEW **2**
1.1 Introduction 2
1.2 Overview 2
Chapter 2. THEORETICAL FOUNDATION **3**
2.1 Fractional calculus in control **3**
2.2 Fractonal-order PID controller **4**
2.3 Decoupling techniques using for multivariable systems **5**
2.3.1 Introduction to decoupling techinques 5
2.3.2 The simplified decoupling method 5
2.4 Smith predictor for multivariable systems **5**
2.5 Identification for multivariable systems **5**
2.5.1 Least squares method for single variable systems 5
2.5.2 Matrix fraction description for multivariable systems 6
Chapter 3. SYSTEM PERFORMANCES AND ROBUST STABILITY **6**
3.1 Performance criteria **6**
3.1.1. IAE index (Integral Abolute Error) 6
3.1.2 ITAE index (Integral of Time-weighted Absolute Error) 6
3.1.3 TV index (Total Variation) 7
3.1.4 Maximum sensitivity function 7
3.2 Robust stability for multivariable systems **7**
3.2.1 Structures for robust stability analysis 7
3.2.2 Robust stability condition using structured singular value (SSV) 7

Chapter 4. THE PROPOSED MEHODS FOR MULTIVARIABLE PROCESSES **7**
4.1 Simplified decoupling combined with Smith predictor **7**
4.2 The particle swarm optimization for model approximation **8**
4.2.1 Introduction to particle swarm optimization 8
4.2.2 Proposing to use PSO for model approximation 8
4.3 The proposed methods to design the fractional-order PI/PID controllers (FOPI/FOPID) **9**
4.3.1 Propose a design method based on internal model control (IMC) 9
4.3.1.1 The tuning rules for some typical processes 9
4.3.1.2 Robust stability analysis for the proposed controller 10
4.3.2 Design PI/PID controllers for high-order multivariable processes using multi-objective optimization 10
4.3.2.1 Multi-objective particle swarm optimization (MOPSO) 10
4.3.2.2 Using MOPSO to design a general-order PI controller 10
4.3.2.3 Robust stability analysis of the multivariable processes 11
Chapter 5. SIMULATION STUDY AND EXPERIMENT **11**
5.1 Simulation studies **11**
5.1.1 The proposed method for TITO processes 11
5.1.1.1 Distillation column Vinante and Luyben (VL) 11
5.1.1.2 Heavy oil fractionator 13
5.1.2 The proposed controller for high-order multivariable processes 14
5.1.2.1 Distillation column Ogunnaike and Ray (OR) 14
5.1.2.2 HVAC for termperature control 16
5.2 The experiment on fractional-order control for multivariable systems **17**
5.2.1 Introduction to the experimental system 18
5.2.2 System identification using the proposed method 18
5.2.3 Controller design 20
Chapter 6. CONCLUSION **23**
6.1. Results **23**
6.2. Limitations and future works **24**
Publications 24
REFERENCES 25

SYMBOLS AND ABBREVIATIONS

- **Format conventions**

Normal letters	function; Ex: min, max, lim, sgn…
Normal and capital lellters in italics	mathematical symbols and operators; Ex: y, α, L, F...
Normal letters in bold	vector; Ex: $\mathbf{g}$, $\mathbf{d}$, $\mathbf{c}$,...
CAPITAL LETTER IN BOLD	matrix; Ex: **A, B, C, G**

- **Symbols**

$D^{-1} f(t)$	Primitive of function $f(t)$
${}_0D_t^{-\alpha} f(t)$	Fractional-order primitive, order of α, of function $f(t)$
${}_0D_t^{\alpha} f(t)$	Fractional-order derivative, order of α, of function $f(t)$
$\Gamma(x)$	Gamma function
$E_\alpha(x),\ E_{\alpha,\beta}(x)$	Mittag-Lefler (M-L) function
$L[.]$	Laplace operator
$F[.]$	Fourier operator
$\mathbf{G}_c(s)$	Closed-loop transfer function matrix
$\mathbf{G}(s)$	Transfer function matrix of multivariable processes
$\hat{\mathbf{G}}(s)$	Estimated transfer function matrix of multivariable processes
$\hat{\mathbf{G}}_0(s)$	Estimated transfer function matrix of multivariable processes, delay times are eliminated
$\mathbf{D}(s)$	Decoupling matrix
$\mathbf{Q}(s)$	Decoupled matrix
$\mathbf{Q}_o(s)$	Decoupled matrix, delay times are eliminated
$\bar{G}(s)$	Approximated transfer function of $G(s)$
q_{ii}	Diagonal elements of matrix **Q**
$\bar{q}_{ii}$	Aproximated transfer function of q_{ii}
q_o	Transfer function of q_{ii}, delay times are eliminated
d_{ij}	Elements of decoupling matrix **D** ($i \neq j$)
g_{ii}	Diagonal elements of matrix **G**
θ	Delay time
$\mu(\mathbf{M})$	μ-synthesis
K_c	Gain of PI/PID controllers
τ_I	Integral time coefficient of PI/PID controllers
K_I	Integral coefficient of PI/PID controllers
τ_D	Derivative time coefficient of PID controllers
K_D	Derivative coefficient of PID controllers
λ	Fractional-order of an integral term
μ	Fractional-order of a derivative term
τ_F	Time constant of a first-order filter

- **Abbreviations**

ARX	Auto Regressive eXternal input
ARMAX	Auto Regressive Moving-Average with eXogenous variable
BJ	Box Jenkins
CM	Coefficient Matching
DRGA	Dynamic Relative Gain Array
DTC	Dead Time Compensator
EA	Evolutionary Algorithm
FO	Fractional Order
FODE	Fractional Ordinary Differential Equation
FOPDT	First Order Plus Delay Time
FOPI/FOPID	Fractional Order Proportional-Integral/Proportional-Integral- Derivative
FOTF	Fractional Order Transfer Function
FSP	Filter Smith Predictor
GA	Genetic Algorithm
HVAC	Heating, Ventilating and Air Conditioning
IMC	Internal Model Control
IO	Integer Order
IRID	Impulse Response Invariant Discretization
LS	Least Squared Method
MFD	Matrix Fraction Description
MIMO	Multi Input Multi Output
MISO	Multi Input Single Output
MOO	Multi-Objective Optimization
MOPSO	Multi-Objective Particle Swarm Optimization
MPC	Model Predictive Control
ODE	Ordinary Differential Equation
OE	Output Error
PEM	Predicted Error Method
PF	Pareto Front
PRBS	Pseudo Random Binary Signal
PSO	Particle Swarm Optimization
RGA	Relative Gain Array
SDSP	Simplified Decoupling Smith Predictor
SP	Smith Predictor
SISO	Single Input Single Output
SOPDT	Second Order Plus Delay Time
SSV	Structured Singular Value
TITO	Two Input Two Output

LIST OF FIGURES

Figure 2.1 Bode plot of Oustaloup approximation 4
Figure 2.2 The decoupling control structure 5
Figure 2.3 Multivariable Smith predictor structure 5
Figure 2.4 Block diagram of discrete linear systems 6
Figure 3.1 The classical control structure 6
Figure 3.2 Geometry illustration of sensitivity function 7
Figure 3.3 Robust stability with multiplicative output uncertainty 7
Figure 3.4 M-Δ structure for robust stability analysis 7
Figure 4.1 The structure of simplified decoupling combined with multivariable Smith predictor 8
Figure 4.2 The structure of the approximation algorithm 9
Figure 4.3 The flowchart of PSO algorithm for model approximation 9
Figure 4.4 M-Δ structure of the proposed controller 10
Figure 4.5 The pseudo-code of the MOPSO algorithm 10
Figure 4.6 The classical closed-loop systems 11
Figure 4.7 The flowchart of the proposed tuning steps 11
Figure 4.8 M-Δ structure for robust stability analysis 11
Figure 5.1 Step responses of q_{11} and its approximation (VL) 12
Figure 5.2 Step responses of q_{22} and its approximation (VL) 12
Figure 5.3a Step responses of control loop 1 (VL) 12
Figure 5.3b Step responses of control loop 2 (tháp VL) 12
Figure 5.4 SSV plots for robust stability (VL) 13
Figure 5.5 Step responses of q_{11} and its approximation (heavy oil) 13
Figure 5.6 Step responses of q_{22} and its approximation (heavy oil) 13
Figure 5.7a Step responses of control loop 1 (heavy oil) 14
Figure 5.7b Step responses of control loop 2 (heavy oil) 14
Figure 5.8 SSV plots for robust stability (heavy oil) 14
Figure 5.9 a, b, and c The obtained PFs using two objective functions J_r and J_d 15
Figure 5.10 a, b, and c. Step responses of control loop 1, 2, and 3 (OR) 15, 16
Figure 5.11. SSV plots for robust stability (OR) 16
Figure 5.12 a, b, c, and d. Step responses of 4 control loops respectively 17
Figure 5.13. SSV plots for robust stability (HVAC) 17
Figure 5.14. Diagram of the quadruple tank system 18
Figure 5.15 (a) The quadruple tank system 18
(b) Block diagram of the controller 18
Figure 5.16 In-out data for loop 1 identification 19
Figure 5.17 In-out data for loop 2 identification 19
Figure 5.18 Validation of identified parameters of loop 1 19

Figure 5.19 Validation of identified parameters of loop 2 20
Figure 5.20 Step responses of $G_{11}(s)$ and its approximation 20
Figure 5.21 Step responses of $G_{12}(s)$ and its approximation 20
Figure 5.22 Step responses of $G_{21}(s)$ and its approximation 20
Figure 5.23 Step responses of $G_{22}(s)$ and its approximation 20
Figure 5.24 Step responses of $q_{11}(s)$ and its approximation 21
Figure 5.25 Step responses of $q_{22}(s)$ and its approximation 21
Figure 5.26 Step responses of control loop 1 21
Figure 5.27 Step responses of control loop 2 21
Figure 5.28 The SSV plots for robust stability (quadruple tank) 22
Figure 5.29 Simulink diagram in real-time control mode 22
Figure 5.30 a, b Step responses of levels in both tanks 22
Figure 5.31 a, b The control voltages of both tanks 22

LIST OF TABLES

Table 4.1 The tuning rules of the proposed controllers for two cases 9
Table 5.1 Performance indices of VL column 13
Table 5.2 Performance indices of heavy oil fractionator 14
Table 5.3 Control parameters and performance indices of OR column 15
Table 5.4 Control parameters and performance indices of HVAC 17
Table 5.5 Performance indices of the quadruple tank system 22

ABSTRACT

Fractional calculus and its applications are interesting problems that attract researchers from many different fields. In the control field, fractional orders of integral and derivative terms are applied in the classical PID controller and extended to a general PID controller, with the order of the derivative and integral terms being real numbers. Many studies have proposed this fractional-order controller, mainly for single-input, single-output systems. Meanwhile, industrial processes are mostly complicated multivariable systems because of the mutual effects of the process variables. As a result of that, controlling these systems is a challenge because it is difficult to manipulate each control loop independently. Various control structures and methods have been proposed, but this is still an open problem that needs to be researched intensively. In this thesis, the author proposes different solutions to solve the problem of multivariable systems using fractional-order controllers. The contributions of the thesis are summarized as follows:

- Propose a new control structure for multivariable processes that combines the simplified decoupling technique and the Smith predictor to deal with delay times in real systems. Although the controller structure is relatively complicated, the system's performance is superior to other methods.

- The simplified decoupling technique of previous research is adopted in this thesis. However, the burden of calculation when deriving each transfer function is still a problem that needs to be solved, especially in the case of a higher order of multivariable processes. Therefore, the author proposed to use particle swarm optimization (PSO) to reduce and simplify the transfer functions of decoupling and decoupled matrices. Using the heuristic method will simplify calculations as well as increase accuracy in the case of higher-order multivariable processes.

- Research fractional calculus and its application in process control, especially the fractional-order PID controller (FOPID). Propose fractional-order controllers and their tuning rules for multivariable controllers. In general, the author proposes two methods: for a 2×2 process using internal model control and for 3×3 and 4×4 processes using multiple objective particle swarm optimization (MOPSO) with an objective function that meets the criteria of system performance and robustness simultaneously. The proposed methods are justified through simulation studies and also compared with other well-known methods using benchmark models in process control.

- Robust stability is an important criterion to prove whether the designed system can be applied in practice. In the thesis, the author uses the **M-Δ** structure and multiplicative output uncertainty to analyze and evaluate the robustness of the proposed controllers. The simulation results prove the robust stability of the proposed methods in comparison with other methods.

- In addition, the applicability of the proposed controller and fractional-order controllers is clarified by experiments using the quadruple tank. The least squares method for identification of single-input, single-output systems is extended to multivariate systems to derive the mathematical model of the tank system, from which the proposed methods are applied to tune the control parameters of the proposed controller. The obtained controllers are adopted to control the system using the Real-Time Window Target of Matlab. The experimental results show that fractional-order controllers can be deployed in practical applications.

TÓM TẮT

Tính toán phân số (fractional calculus) và các ứng dụng của nó là vấn đề mới thu hút nhiều nhà nghiên cứu từ nhiều lĩnh vực khác nhau. Trong lĩnh vực điều khiển, tích phân và đạo hàm bậc phân số được ứng dụng trong bộ điều khiển PID cổ điển và mở rộng nó thành bộ điều khiển PID tổng quát với bậc của đạo hàm và tích phân là số thực. Nhiều công trình nghiên cứu đã đề xuất bộ điều khiển bậc phân số này nhưng chủ yếu cho hệ đơn biến. Trong khi đó, các quá trình công nghiệp hầu hết là hệ đa biến phức tạp vì sự ảnh hưởng lẫn nhau giữa các biến có trong hệ thống. Do đó, điều khiển những hệ thống này là bài toán phức tạp vì khó có thể hiệu chỉnh từng vòng điều khiển độc lập. Nhiều cấu trúc cũng như các phương pháp điều khiển khác nhau đã được đề xuất, nhưng đây vẫn là bài toán mở cần tập trung nghiên cứu. Trong luận án này tác giả đề xuất các giải pháp khác nhau để giải quyết bài toán hệ đa biến sử dụng bộ điều khiển bậc phân số. Các đóng góp của luận án được tóm tắt như sau:

- Đề xuất cấu trúc điều khiển mới cho hệ đa biến trong đó kết hợp cả kỹ thuật phân ly đơn giản hóa cho hệ đa biến và bộ dự báo Smith nhằm đối phó với các khâu trễ hiện hữu trong các hệ thống thật. Mặc dù cấu trúc bộ điều khiển tương đối phức tạp, nhưng hiệu quả mang lại tốt hơn hẳn khi so sánh với các phương pháp khác.
- Kỹ thuật phân ly đơn giản hóa của các nghiên cứu trước được sử dụng trong luận án. Tuy nhiên, việc tính toán và rút gọn các hàm truyền thành phần vẫn là vấn đề cần giải quyết, đặc biệt khi bậc của hệ đa biến tăng cao. Do đo, tác giả đề xuất sử dụng giải thuật tối ưu hóa bày đàn (PSO) trong việc rút gọn và đơn giản hóa các hàm truyền thành phần của ma trận phân ly cũng như ma trận sau khi phân ly. Sử dụng thuật toán tiến hóa sẽ đơn giản hóa việc tính toán và tăng độ chính xác khi bậc của hệ đa biến tăng cao.
- Nghiên cứu tính toán phân số (fractional calculus) và ứng dụng trong lĩnh vực điều khiển, đặc biệt là bộ điều khiển PID bậc phân số. Đề xuất bộ điều khiển phân số và các phương pháp hiệu chỉnh thông số cho các bộ điều khiển đa biến. Cụ thể, tác giả đề xuất 2 phương pháp hiệu chỉnh: cho hệ bậc thấp (2×2) sử dụng cấu trúc mô hình nội và cho hệ bậc cao (3×3, và 4×4) sử dụng tối ưu hóa bày đàn đa mục tiêu (MOPSO) với hàm mục tiêu đảm bảo tiêu chí đáp ứng đồng thời bộ điều khiển phải có sự ổn định bền vững. Các phương pháp đề xuất đều được kiểm chứng thông qua việc mô phỏng và so sánh với các phương pháp khác đã được công bố sử dụng các mô hình chuẩn thường được nghiên cứu trong lĩnh vực điều khiển quá trình.
- Sự ổn định bền vững là một tiêu chí quan trọng minh chứng cho việc hệ thống thiết kế có thể ứng dụng trong thực tế hay không. Trong luận án, tác giả sử dụng cấu trúc **M-Δ** và sai số nhân đầu ra (multiplicative output uncertainty) để phân tích, đánh giá ổn định bền vững cho các bộ điều khiển đề xuất. Kết quả mô phỏng đều minh chứng được sự ổn định bền vững khi so sánh với các nghiên cứu khác.
- Bên cạnh đó, khả năng ứng dụng thực tế của bộ điều khiển đề xuất cũng như điều khiển bậc phân số cũng được làm rõ bằng thực nghiệm sử dụng hệ bốn bồn nước liên kết (quadruple tank). Phương pháp bình phương tối thiểu trong nhận dạng hệ đơn biến được mở rộng sang nhận dạng hệ đa biến và ứng dụng để nhận dạng và mô hình hóa hệ bồn nước, từ đó áp dụng các phương pháp đề xuất để tìm thông số bộ điều khiển tương ứng. Bộ điều khiển tìm được được áp dụng điều khiển trực tiếp hệ thống thật ở chế độ thời gian thực của Matlab (Real Time Window Target). Kết quả thực nghiệm chứng tỏ phương pháp điều khiển bậc phân số có thể áp dụng vào điều khiển vào các ứng dụng trong thực tế.

INTRODUCTION

1. Problem statement

The centralized control method with multi-loop PI/PID controllers is often used for multivariable processes with low interaction (interaction between process variables is negligible) because of its simple structure, efficiency, and appropriate performance. However, these controllers often perform poorly when interaction increases significantly. In that case, some advanced control algorithms are used, such as model predictive control (MPC), fuzzy control, neural networks, etc. However, they face many difficulties in real-time implementation.

Therefore, decentralized control with decoupling techniques attracts many researchers. The decoupling technique is used to minimize interactions between variables in the system, and as a result, simple independent control loops can be designed. That means, from a multivariable system with many inputs and outputs, we convert it into many single-variable systems. In addition, time delay is also an existing feature in process control systems. The delay time will cause difficulties in analyzing the characteristics and designing a controller for the system, especially in multivariable systems with different delay times, as well as adversely affect the response in most cases. This thesis will also set a new approach when designing PID controllers, which is fractional-order control based on the mathematical foundation of fractional calculus.

Another important aspect when designing a controller in an application is system modeling. In this study, the author will also extend an identification technique for single-variable systems to use for multivariable processes.

2. Research goals

Based on the issues mentioned above, in this thesis, the author will focus on researching the following contents:

- Proposing a solution to improve the calculation method of the simplified decoupling technique.
- Proposing a new control structure for multivariable systems to improve the response of the system not only when the set-point changes but also when affected by process disturbances. In addition, it is also possible to eliminate the influence of delay times on the process. Evaluate the robust stability of the proposed control structure.
- Research on fractional-order PID controllers is based on the mathematical foundation of fractional calculus. Proposing a new method to design a fractional-order PID controller for multivariable systems.
- Build an experimental model to verify the proposed method. Propose a method to identify parameters of multivariable systems to obtain mathematical equations of the experimental model for the design and evaluation of the proposed methods.

3. Research scopes

- In this thesis, the author limits the study to square multivariable systems represented by a $n \times n$ matrix.
- Regarding theoretical research on multivariable systems, the author will generalize to n-order systems. However, in the simulation study, the author only mentions 2×2, 3×3, and 4×4 systems, which are common systems in the field of process control. In the experiment, due to equipment limitations, the author only tests on the 2×2 system.

4. Research approach and methods

To ensure the novelty of the research, the author will review recent related works from prestigious international journals in the field of research. The proposed method will also be simulated and compared with other outstanding methods from works in prestigious journals. In addition, an experimental model will also be built to demonstrate the practical applicability of the proposed methods.

5. Scientific and practical contributions

The achieved results are summarized into the following main contents:

▪ ***Scientific contributions:***

- *Analyzing the necessity of fractional order in describing the dynamics of systems*. From there, the necessity of fractional calculus in the control field is also explained. *Research the effects of fractional-order derivatives and integrals* on control signals in classical feedback controllers. The simulation results show that the fractional-order controller makes the control signal flexible, less affected by disturbances, and also makes the entire control system more robust.

- Using the simplified decoupling technique proposed by Vu and Lee, *the author has successfully proposed the use of the PSO algorithm to simplify* the component transfer functions of the decoupling and decoupled matrix. This is to simplify calculations when the order of the system increases. The achieved results demonstrate that the proposed method gives better approximations than the ones in previous publications.

- Proposing a new control structure for multivariable systems that combines the simplified decoupling technique and the Smith predictor. Although the controller structure is relatively complicated, the performance is better when compared with other methods.

- Research fractional calculus and applications in the field of control, especially the fractional-order PID controller (FOPID). Proposing fractional controllers and parameter tuning methods for multivariable controllers. The author proposes two specific methods:

  - ✓ For 2×2 multivariable systems, use the internal model control (IMC) with the proposed fractional controller. To find the parameters of the controller, the author tunes via the desired response time constant to compromise between the system response to the servomechanism problem (set-point changes) and the regulator problem (disturbance changes).
  - ✓ With higher-order multivariable systems (3×3 and 4×4), use multi-objective swarm optimization (MOPSO) to find control parameters with the objective function that minimizes the error when both the set-point and disturbance change. The feasible solutions of the optimization problem will converge on the Pareto front, and from there, the appropriate solutions (control parameters) will be selected through the value of the maximum sensitivity function M_s to ensure the robust stability of the control systems.

- The proposed methods are verified through comparison with other published methods using benchmark models commonly researched in the field of process control.

▪ ***Practical contributions:***

- The design methods proposed in the thesis are model-based design methods, so finding the mathematical model of the process is essential. However, in reality, there is always a mismatch between the obtained model and the actual model of the system, leading to the design method not being applicable in practice. Therefore, robust stability is an important criterion that demonstrates the applicability of the control system. In the thesis, the author uses the **M-Δ** structure and multiplicative output uncertainty to analyze and evaluate the robustness of the proposed control methods. Simulation results demonstrate the robust stability of the proposed methods, meaning they have high applicability.

- Research on identification methods for multivariable systems by using the matrix fraction description (MFD) technique to convert MIMO systems into multiple-input, single-output (MISO) systems. From there, we can apply the common identification technique for single-variable systems (the least squares method) to identify multivariable systems. Applying the proposed method to identify the model of the quadruple tank.

- The design method for the fractional-order controller is experimentally verified for the quadruple tank with a 2×2 transfer function matrix. The control results clearly demonstrate the practical applicability of fractional-order control as well as the proposed design method. In the world, the field of multivariable system control is widely applied in distillation column systems and production processes, bringing great economic benefits. The proposed method has also demonstrated high applicability, so if implemented in practice, it will have great practical significance.

6. Thesis structure: The thesis is presented in 6 chapters, including figures, tables and appendices.

Chapter 1. OVERVIEW

1.1. Introduction

Fractional calculus has been around for a long time. However, the application of fractional computation in control has only developed in the last two decades. In particular, Podlubny proposed the fractional-order PID controller as a general case of the classical PID controller. The controller parameters are added with two additional coefficients: orders of the derivative and the integral terms (fractional order). This is a new research field in control engineering with many open problems, and that is also the approach of the thesis, which is *fractional-order control* based on fractional calculus.

1.2. Overview

An overview of the research and development of fractional-order control is presented in detail in the thesis, from references [1–47]. The references [48–100] are reviews of research on methods of controlling multivariable systems as well as methods of designing integer or fractional-order PID controllers applied to multivariable systems.

According to the author's review, up to the time of the study, the structure of the decoupling controller combined with the multivariable Smith predictor had not been studied. Therefore, in this thesis, the author proposes to use this structure to control multivariable systems. In addition, research on fractional-order PI/PID controllers (FOPI/FOPID) for multivariable systems is very limited, and if there is, most of them only deal with the 2×2 systems. Typical related works are articles [85, 98, 100]. The work [85] uses inverted decoupling combined with a FOPID controller designed according to the IMC structure. The results have only been verified for some processes proposed by the authors and lack objective comparison with other methods. The article [100] applies the FOPI controller to a coupled-tank system (TITO); however, the approach is not suitable for higher-order systems when combining feedback and feedforward control. The article [98] uses centralized control combined with a simplified decoupling technique for a 2×2 system. Regarding the controller, the authors used the search algorithm method, the dynamic bat algorithm, to design the FOPID controller. In fact, these evolutionary techniques should only be used for systems that can not be completely solved by conventional methods (such as high-order multivariable systems). Therefore, the controller structure commonly used in the thesis is called the simplified decoupling technique combined with the Smith predictor using a fractional order controller (F-SDSP).

The analytical tuning rules of the proposed controllers use both the internal model control (IMC) for the lower-order multivariable system (2×2) and the search algorithm for the higher-order systems (3×3 and 4×4), specifically the multi-objective optimization algorithm using swarm optimization (MOPSO). To evaluate the robust stability of the entire control system, the **M-Δ** structure commonly used for systems with integer order is also extended to be used for systems with fractional order.

Chapter 2. THEORETICAL FOUNDATION

2.1 Fractional calculus in control

There are many different definitions of fractional integrals and derivatives. However, the most commonly used definition is that of Riemann-Liouville, for details we can refer to references [9–13]

❖ **Definition 2.1:** *definition Riemann-Liouville (R-L) of fractional integrals.*

$$ {}_0D_t^{-\alpha} f(t) = \frac{1}{\Gamma(\alpha)} \int_0^t \frac{f(\tau)}{(t-\tau)^{1-\alpha}} d\tau \tag{2.1}$$

where, $0<\alpha<1$ and $\Gamma(x)$ is Gamma function, where $\Gamma(x)=\int_0^\infty e^{-u}u^{x-1}du$ (2.2)

❖ **Definition 2.2:** *definition Riemann-Liouville (R-L) of fractional derivatives.*

Definition R-L of fractional derivatives based on fractional integrals:

$$ {}_0D_t^{\alpha} f(t) = \frac{d}{dt}\left[{}_0D_t^{-(1-\alpha)} f(t) \right] \tag{2.3} $$

❖ **Laplace and Fourier transform**

Laplace and Fourier transforms are basic and important tools of control engineering. Details of these transformations can be referred to [10].

❖ **Fractional ordinary differential equation**

Fractional ordinary differential equation (FODE) is the basis for describing the dynamics of fractional-order systems. The fractional difference equation is described by equation (2.4):

$$ a_n D^{\alpha_n} y(t) + a_{n-1} D^{\alpha_{n-1}} y(t) + \ldots + a_0 D^{\alpha_0} y(t) = b_m D^{\beta_m} u(t) + \ldots + b_0 D^{\beta_0} u(t) \tag{2.4} $$

where: $a_0 \ldots a_n;\ b_0 \ldots b_m$ are constants

$\alpha_0 < \ldots < \alpha_{n-1} < \alpha_n;\ \beta_0 < \ldots < \beta_m$ are positive real numbers

Nếu α_i và β_j are integer multiples of a base order, the system will be commensureate order and if there is no common coefficient, it is called non-commensurate order.

❖ **Fractional-order transfer function**

From (2.4) and using Laplace transform (initial conditions equal to 0), we have fractional-order transfer function:

$$ G(s) = \frac{b_m s^{\beta_m} + \ldots + b_0 s^{\beta_0}}{a_n s^{\alpha_n} + a_{n-1} s^{\alpha_{n-1}} + \ldots + a_0 s^{\alpha_0}} \tag{2.5} $$

❖ **Fractional-order approximation in frequency domain**

Oustaloup approximation is described by the following equation:

$$ s^{\alpha} \cong s^{\alpha}_{[\omega_l, \omega_h]} \approx K \sum_{k=-N}^{N} \frac{s + \omega'_k}{s + \omega_k} \tag{2.6} $$

where, α is the non-integer degree ($\alpha \in R^+$); $[\omega_l,\ \omega_h]$ is the approximate frequency range; K is the adjustment parameter so that both sides of the above equation have a gain of 1 at the cut-off frequency, easily seen as $\omega_c = 1$ rad/s ; N is the number of pole/zero roots (usually N is chosen from 3 to 8). Usually, ω_l, ω_h are chosen as $0.001\omega_c$ and $1000\omega_c$ respectively. The gain, zero and pole are calculated by the following formulas

$$ K = \omega_h^{\alpha} $$

$$ \omega'_k = \omega_l \left(\frac{\omega_h}{\omega_l} \right)^{(k+N+0.5-0.5\alpha)/(2N+1)} $$

$$ \omega_k = \omega_l \left(\frac{\omega_h}{\omega_l} \right)^{(k+N+0.5+0.5\alpha)/(2N+1)} $$

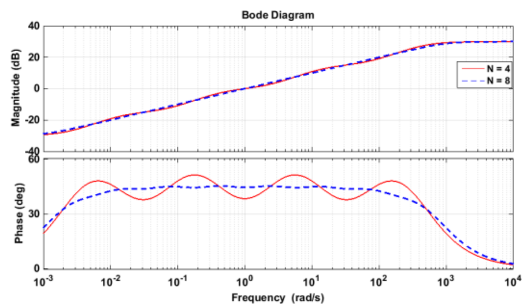

Figure 2.1 Bode plot of Oustaloup approximation

Figure 2.1 illustrates the Bode plot of $s^{0.5}$ in the frequency range $[10^{-3},\ 10^{4}]$ (rad/s) using Oustaloup's approximation method. The number of pole/zero is chosen in two cases N = 4 and N = 8. To increase calculation speed, in this thesis, the author choses N = 5.

2.2 Fractional-order PID controller

Fractional-order PID controller, $\mathrm{PI}^{\lambda}\mathrm{D}^{\mu}$, proposed by Podlubny [15]. Its transfer function has the following form:

$$ G_c(s) = K_P + \frac{K_I}{s^{\lambda}} + K_D s^{\mu} \qquad (\lambda, \mu \geq 0) \tag{2.7} $$

where: K_P, K_I, K_D are coefficients of proportional, integral and derivative respectively; λ, μ are the fractional orders of integral and derivative term respectively. It is obvious that if $\lambda = 1,\ \mu = 1$ it becomes the classical PID controller.

2.3 Decoupling techniques using for multivariable systems

2.3.1 Introduction to decoupling techniques

Consider the decoupling control system shown in Figure 2.2, where $\mathbf{G}_c$ is the closed-loop controller, **D** is the decoupling matrix. **G** and **Q** are the multivariable process and the decoupled multivariable process, respectively.

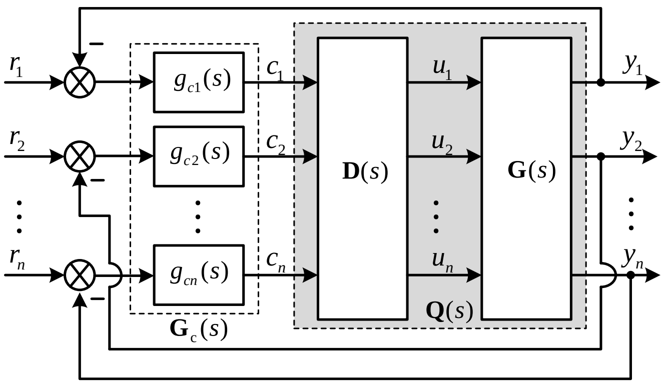

Figure 2.2 The decoupling control structure

The objective of a decoupling technique is to determine the decoupling matrix **D**, such that **G**(s)**D**(s) = **Q**(s), is a diagonal matrix.

$$\begin{bmatrix} g_{11} & \cdots & g_{1n} \\ \vdots & \ddots & \vdots \\ g_{n1} & \cdots & g_{nn} \end{bmatrix} \begin{bmatrix} d_{11} & \cdots & d_{1n} \\ \vdots & \ddots & \vdots \\ d_{n1} & \cdots & \mathrm{d}_{nn} \end{bmatrix} = \begin{bmatrix} q_{11} & \cdots & 0 \\ \vdots & \ddots & \vdots \\ 0 & \cdots & q_{nn} \end{bmatrix} \tag{2.8}$$

There are three decoupling techniques, but in this thesis, the simplified decoupling technique is adopted (the rationale is analyzed in the thesis). In that case, the diagonal elements of decoupling matrix equal to unit, $d_{ii} = 1$, i =1÷n

2.3.2 The simplified decoupling method

In general, elements (i, j) of decoupling matrix **D**(s) can be determined as follows:

$$d_{ji} = d_{ii}\frac{c_{ij}}{c_{ii}}, \quad i, j = 1, 2, \ldots, n; \; i \neq j \tag{2.9}$$

The diagonal elements of decoupled matrix can be calculated as follows:

$$q_{ii} = d_{ii}\frac{g_{ii}}{\Lambda_{ii}} \tag{2.10}$$

where, **C** = (adj**G**)^T and $\Lambda_{ii} = \left[\mathbf{G} \otimes \left(\mathbf{G}^{-1}\right)^T\right]_{ii} = g_{ii}\dfrac{c_{ii}}{|\mathbf{G}|}$ where $\otimes$ is element product.

2.4 Smith predictor for multivariable systems

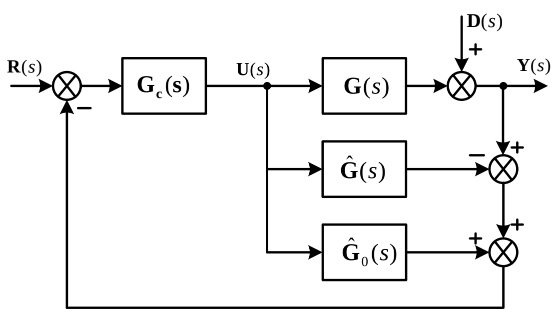

Figure 2.3. Multivariable Smith predictor structure

Figure 2.3 describes the controller structure using Smith predictor for multivariable systems. Then, the closed-loop transfer function matrix between output **Y**(s) and input **R**(s) is as follows:

$$\mathbf{H}(s) = \hat{\mathbf{G}}(s)\hat{\mathbf{G}}_0^{-1}(s)\hat{\mathbf{G}}_0(s)\mathbf{G}_c(s)\left[\mathbf{I} + \hat{\mathbf{G}}_0(s)\mathbf{G}_c(s)\right]^{-1}$$

$$\Rightarrow \mathbf{H}(s) = \hat{\mathbf{G}}(s)\hat{\mathbf{G}}_0^{-1}(s)\mathbf{H}_0(s) \tag{2.11}$$

where, $\mathbf{H}_0(s) = \hat{\mathbf{G}}_0(s)\mathbf{G}_c(s)\left[\mathbf{I} + \hat{\mathbf{G}}_0(s)\mathbf{G}_c(s)\right]^{-1}$ (2.12)

$\mathbf{H}_0(s)$ is closed-loop transfer function with non-delay process $\mathbf{G}_0(s)$

2.5 Identification for multivariable systems

Overviews of research on system identifications are presented in the thesis, from references [116 - 138]. In this thesis, the author uses well-known identification techniques for single-variable systems, the least squares (LS) method, and extends it to apply to multivariable systems.

2.5.1. Least squares method for single variable systems

The block diagram of the discrete single variable linear system is shown in Figure 3.1, where z is the discrete operator; θ is the delay time. The linear differential equation of a discrete, linear and invariant system has the following form:

$$y(t_k) + a_1 y(t_{k-1}) + \ldots + a_{n_a} y(t_{k-n_a}) = b_1 u(t_{k-1}) + \cdots + b_{n_b} u(t_{k-n_b}) + v(t_k) \quad (2.13)$$

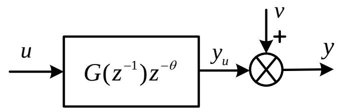

Figure 3.1. Block diagram of discrete linear systems

Equation (2.13) can be expressed in vector form according to the linearity of the model parameters:

$$y(t_k) = \boldsymbol{\varphi}^T(t_k)\boldsymbol{\theta} + v(t_k) \quad (2.14)$$

where: $\boldsymbol{\varphi}^T(t_k) = \left[-y(t_{k-1})\ldots - y(t_{k-n_a})\ u(t_{k-1})\ldots u(t_{k-n_b})\right]$: ***regressor vector***

$\boldsymbol{\theta} = \left[a_1 \ldots a_{n_a}\ b_1 \ldots b_{n_b}\right]^T$: ***vector of system parameters***

Using well-know least squares method, we obtain the solution of Eq. (2.14):

$$\hat{\boldsymbol{\theta}}_{LS} = \left[\frac{1}{N}\sum_{k=1}^{N}\boldsymbol{\varphi}(t_k)\boldsymbol{\varphi}^T(t_k)\right]^{-1}\frac{1}{N}\sum_{k=1}^{N}\boldsymbol{\varphi}(t_k)y(t_k) \quad (2.15)$$

2.5.2 Matrix fraction description for multivariable systems

For identification purpose, another form of MIMO normally uses as follows:

$$y(t) + \mathbf{A}_1 y(t-1) + \ldots + \mathbf{A}_k y(t-k) = \mathbf{B}_0 u(t) + \mathbf{B}_1 u(t-1) + \ldots + \mathbf{B}_k u(t-k) \quad (2.16)$$

where: $\mathbf{A}_1(n\times n),\ldots,\ \mathbf{A}_n(n\times n),\ \mathbf{B}_0(m\times n),\ \mathbf{B}_1(m\times n),\ldots,\ \mathbf{B}_n(m\times n)$: are constant matrix

Representing a transfer function matrix by two polynomial matrices is called matrix fraction description (MFD). To ensure uniqueness of the identified model, the simplest form of MFD is used, which is the diagonal form.

$$\mathbf{A}(q) = \begin{bmatrix} A_{11}(q) & 0 & \ldots & 0 \\ 0 & A_{22}(q) & \ldots & \vdots \\ \vdots & \vdots & \ddots & 0 \\ 0 & \ldots & \ldots & A_{nn}(q) \end{bmatrix},\ \mathbf{B}(q) = \begin{bmatrix} B_{11}(q) & B_{12}(q) & \ldots & B_{1m}(q) \\ B_{21}(q) & B_{22}(q) & \ldots & B_{2m}(q) \\ \vdots & \vdots & \ddots & \vdots \\ B_{n1}(q) & B_{n2}(q) & \ldots & B_{nm}(q) \end{bmatrix} \quad (2.17)$$

where $A_{11}(q),\ \ldots, A_{nn}(q)$ are polynomials with a coefficient of highest order equals to 1, and the orders of polynomial $B_{i1}(q),\ \ldots B_{im}(q)$ are less than or equal to the order of $A_{ii}(q)$.

This method is simple and a MIMO system becomes MISO systems. Thereofore, the complex of multivariable systems especially high-order system, will be minimized.

Chapter 3. SYSTEM PERFOMANCES AND ROBUST STABILITY

3.1 Performance criteria

Consider the classical feedback systems shown in Figure 3.1. To evaluate the performance of the proposed method, in this thesis, the following performance indices will be considered.

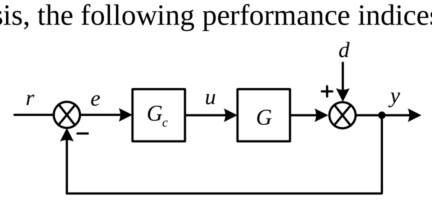

Figure 3.1. The classical control structure.

3.1.1. IAE index (Integral Absolute Error)

$$\text{IAE} = \int_0^T |e(t)|\,dt \approx \sum_{k=1}^{N}|e_k| \quad (3.1)$$

where, T is a specific time and is chosen as the simulation time. From IAE index, we also have other indices:

- J_r: is IAE index when the set-point (r) is changed.
- J_d: is IAE index when disturbance (d) is inserted to the control loop.

3.1.2. ITAE index (Integral of Time-weighted Absolute Error)

$$\text{ITAE} = \int_0^T t\left|e(t)\right|dt \approx \sum_{k=1}^{N} t_k \left|e_k\right| \tag{3.2}$$

3.1.3. TV index (Total Variation)

To evaluate the amplitude as well as the amount of change of the control signal, TV index is often used:

$$\text{TV} = \sum_{k=1}^{N}\left|u(k+1) - u(k)\right| \tag{3.3}$$

3.1.4. Maximum sensitivity function

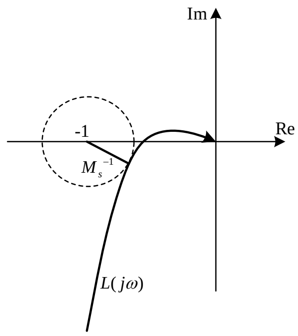

Figure 3.2. Geometry illustration of sensitivity function

From figure 3.1, the open loop transfer function is $L = GG_c$. In the frequency domain, $L(j\omega)$, we have a formula to obtain the maximum sensitivity function:

$M_s = \max_{\omega \to \infty}\left|S(j\omega)\right|$, where $S(j\omega) = \left(1 + L(j\omega)\right)^{-1}$
(3.4)(3.4)

In figure 3.2, M_s is the inverse of the shortest distance from the Nyquist of $L(j\omega)$ to the critical point (-1, j0) in the complex plane. To guarantee the robust stability of the closed-loop system, the typical range of M_s is 1.2 ÷ 2 [139].

3.2 Robust stability for multivariable systems

3.2.1. Structure for robust stability analysis

To analyze robust stability of a control system (figure 3.3), the **M-Δ** structure as figure 3.4 is addressed. If the nominal system is stable, then **M** will be stable and **Δ** is uncertainties that can make the system unstable.

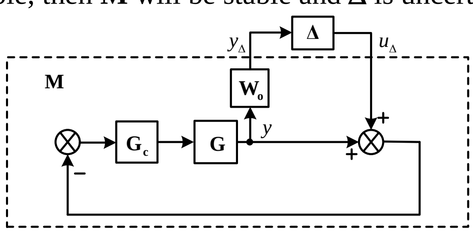

Figure 3.3. Robust stability with multiplicative output uncertainty

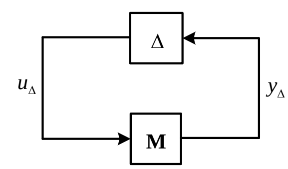

Figure 3.4: M-Δ structure for robust stability analysis

3.2.2 Robust stability condition using structured singular value (SSV)

- **Definition (SSV):** *Given matrix **M** and* $\mathbf{\Delta} = diag\{\Delta_i\}$ *where* $\bar{\sigma}(\mathbf{\Delta}) \le 1$. *The positive semidefinite function* $\mu(\mathbf{M})$ *is called SSV and its definition is as follows:*

$$\mu(\mathbf{M}) \triangleq \frac{1}{\min\left\{k_m \middle| \det\left(\mathbf{I} - k_m \mathbf{M}\Delta\right) = 0,\ \bar{\sigma}(\Delta) \le 1\right\}} \tag{3.5}$$

If no Δ *structure exits,* $\mu(\mathbf{M}) = 0$

- **Theorem:** *Assume that the nominal model **M** and the uncertainty signal* $\mathbf{\Delta}$ *are stable. Then the structure **M-***$\mathbf{\Delta}$ *in figure 3.4 is also stable for all* $\mathbf{\Delta}$ *with* $\bar{\sigma}(\mathbf{\Delta}) \le 1,\ \forall\omega$ *if and only if:* $\mu\left(\mathbf{M}(j\omega)\right) < 1\ \ \forall\omega$

where, $\mathbf{M(s)} = -\mathbf{W_o G G_c}\left[\mathbf{I} + \mathbf{G G_c}\right]^{-1}$ (3.6)

Chapter 4. THE PROPOSED METHODS FOR MULTIVARIABLE PROCESSES

4.1 The combination of simplified decoupling with Smith predictor

The general structure of the controller is described in Figure 4.1. In which, **D**(s) is the decoupling matrix for the multivariable process **G**(s), **Q**(s) is the decoupled process matrix (**Q**(s) = **G**(s)**D**(s)) and $\mathbf{Q_0}(s)$ is derived from **Q**(s) when all delay times are removed.

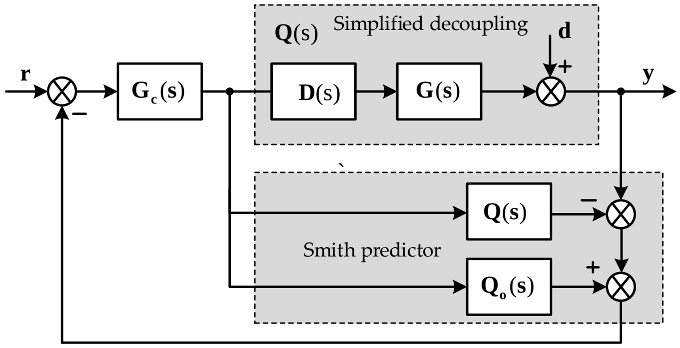

Figure 4.1: The structure of simplified decoupling combined with multivariable Smith predictor

$$\mathbf{G}_c(s)=\begin{bmatrix} g_{c1}(s) & 0 & \dots & 0 \\ 0 & g_{c2}(s) & \dots & 0 \\ \vdots & \vdots & \vdots & \vdots \\ 0 & 0 & \dots & g_{cn}(s) \end{bmatrix} \tag{4.1}$$

$$d_{ji}=\frac{c_{ij}}{c_{ii}}, \quad i,j=1,2,\dots,n;\ i\neq j \tag{4.2}$$

$$q_{ii}=\frac{g_{ii}}{\Lambda_{ii}} \tag{4.3}$$

Where, $\mathbf{C}$ = $(adj\mathbf{G})^T$ and $\Lambda_{ii}=\left[\mathbf{G}\otimes(\mathbf{G}^{-1})^T\right]_{ii}$

$\otimes$ is the element product of matrices.

The diagonal components of the decoupling and decoupled matrix are very complex and can not be used for controller design. In this thesis, the author has proposed a method of using the swarm optimization algorithm (PSO) to approximate the above components to simple and common forms in the field of process control.

4.2. The swarm optimization algorithm to approximate models

4.2.1. Introduction to swarm optimization algorithm

At each step, all individuals are updated with two best values: the individual best position (*Pbest*) and the group's best position (*Gbest*) up to the current step. The well-known equations used to update the position and velocity of each individual are as follows:

$$v_i(k+1)=\omega v_i(k)+c_1\omega_1\left(x_{Pbest}-x_i(k)\right)+c_2\omega_2\left(x_{Gbest}-x_i(k)\right) \tag{4.4}$$

$$\omega=\omega_{\max}-\frac{\omega_{\max}-\omega_{\min}}{M}k;\ x_i(k+1)=x_i(k)+v_i(k+1) \tag{4.5}$$

Where, $v_i(k)$ and $x_i(k)$ are velocity and position of the i^{th} indivitual; k is iteration step; c_1 and c_2 are accerleration coefficients or learning coefficients; ω_1 and ω_2 are real numbers which randomly generate in range of [0–1]; ω is the inertial weight; *M* is maximum iteration.

4.2.2 Proposing to use PSO to approximate models

The integer-order and fractional-order transfer functions are suggested to approximate the complex ones:

$$G_m(s)=\frac{K(\tau_3 s+1)e^{-\theta s}}{(\tau_1 s+1)(\tau_2 s+1)};\ G_m(s)=\frac{Ke^{-\theta s}}{\tau_2 s^{\alpha_2}+\tau_1 s^{\alpha_1}+1} \qquad \left(0<\alpha_1\le 1<\alpha_2<2\right) \tag{4.6}$$

Where, τ_1 and τ_2 are time constants, without loss of generality, assuming $\tau_1>\tau_2\ge 0$; K is gain; τ_3 is non-negative, when $\tau_3=0$ the above transfer function becomes second order plus delay time (SOPDT), and $\tau_2=0$ simultaneously, the transfer function becomes first order plus delay time (FOPDT); θ is delay time; α_2, α_1 are fractional order.

For integer transfer functions, from the general transfer function (4.6), we can obtain a number of transfer functions such as: first order plus delay time (FOPDT), second order plus delay time (SOPDT) and second order plus delay time with negative zero (SOPTDNZ) as equation (4.7)

$$\bar{G}_m(s)=\frac{Ke^{-\theta s}}{\tau s+1} \qquad \bar{G}_m(s)=\frac{Ke^{-\theta s}}{(\tau_1 s+1)(\tau_2 s+1)} \qquad \bar{G}_m(s)=\frac{K(\tau_3 s+1)e^{-\theta s}}{(\tau_1 s+1)(\tau_2 s+1)} \tag{4.7}$$

Similar to fractional-order transfer fucntions, afer approximation, we have some following forms:

$$\bar{G}_m(s) = \frac{Ke^{-\theta s}}{\tau s^{\alpha} + 1} \qquad \left(0 < \alpha < 1\right) \qquad (4.8); \qquad \bar{G}_m(s) = \frac{Ke^{-\theta s}}{\tau_2 s^{\alpha_2} + \tau_1 s^{\alpha_1} + 1} \qquad \left(0 < \alpha_1 \le 1 < \alpha_2 < 2\right) \qquad (4.9)$$

The approximation algorithm is described as follows:

The parameters θ , $K_{\min}$, $K_{\max}$ and $\tau_{i\max}$ $(i = 1 \div 3)$ are determined based on open loop response with step function input.

$$\mathbf{x} = \left[K \quad \tau_1 \quad \tau_2 \quad \tau_3 \quad \alpha_1 \quad \alpha_2\right]^T$$

$$\begin{cases} K_{\min} < K < K_{\max} \\ 0 < \tau_1 < \tau_{1\max} \\ 0 \le \tau_2 < \tau_{2\max} \\ 0 \le \tau_3 < \tau_{3\max} \\ 0 < \alpha_1 \le 1 \\ 1 < \alpha_2 < 2 \end{cases} \qquad (4.10)$$

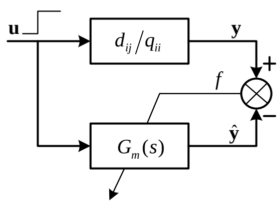

Figure 4.2. The structure of the approximation algorithm

The objective function: $$f = \frac{1}{N}\sum_{i=1}^{N}\left(y - \hat{y}\right)^2 \qquad (4.11)$$

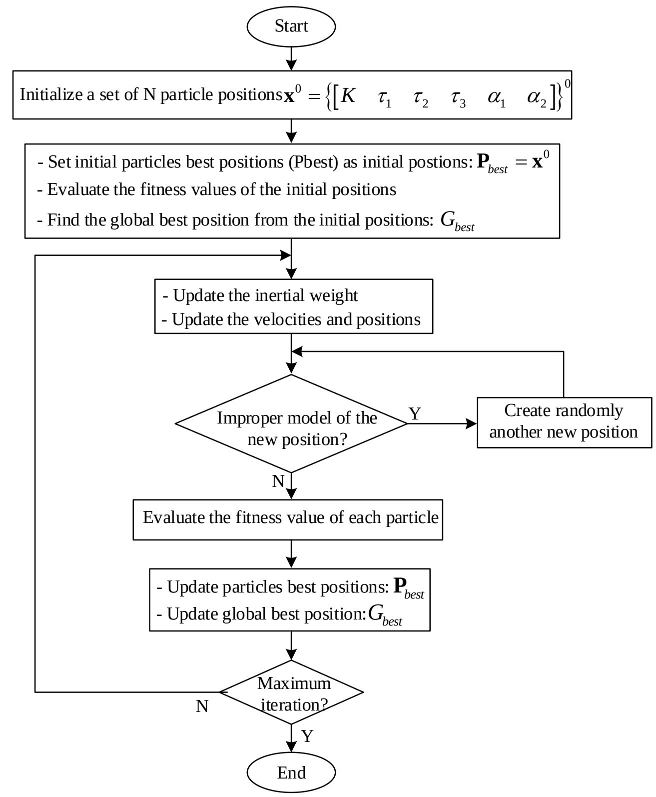

Figure 4.3. The flowchart of PSO algorithm for model approximation

4.3. The proposed method to design the fractional-order PI/PID controllers (FOPI/FOPID)

In this thesis, the author proposes a novel structure of a fractional-order PID, called $\mathrm{I}^{\sigma}\,\mathrm{PI}^{\lambda}\,\mathrm{D}^{\mu}$ controller. The general transfer function has the following form:

$$g_c(s) = K_c \frac{1}{s^{\sigma}}\left(1 + \frac{1}{\tau_I s^{\lambda}} + \tau_D s^{\mu}\right)\frac{1}{\tau_F s + 1} \qquad (4.12)$$

Where, K_c, τ_I, τ_D are gain, integral time, derivative time respectively; λ, μ are fractional order of the integral and derivative term respectively; σ is fractional order of ideal integral term, and: $\sigma = 1 - \lambda$. In special case, $\lambda = 1$, we will have $\sigma = 0$; τ_F is time constant of the first-order lowpass filter, in case of no filter $\tau_F = 0$.

4.3.1 Propose a design method based on internal model control (IMC)

4.3.1.1. The tuning rules for some typical processes

Table 4.1. The tuning rules of controllers for some cases

Models	The tuning rules of controllers
$\bar{q}_o(s) = \dfrac{K}{\tau s^{\alpha} + 1}$ $(0 < \alpha < 1)$	$K_c = \dfrac{\tau}{K\tau_c}$; $\tau_I = \tau$; $\lambda = \alpha$; $\sigma = 1 - \alpha$ $\tau_D = \tau_F = 0$
$\bar{q}_0(s) = \dfrac{K}{\tau_2 s^{\alpha_2} + \tau_1 s^{\alpha_1} + 1}$ $(0 < \alpha_1 \le 1 < \alpha_2 < 2)$	$K_c = \dfrac{\tau_1}{2K\tau_c}$; $\tau_I = \tau_1$; $\tau_D = \dfrac{\tau_2}{\tau_1}$; $\lambda = \alpha_1$; $\sigma = 1 - \alpha_1$

	$\mu = \alpha_2 - \alpha_1$; $\tau_F = \dfrac{\tau_c}{2}$

4.3.1.2. Robust stability analysis for the proposed controller.

The proposed controller (figure 4.1) is equivalently transformed to **M-Δ** structure as figure 4.4.

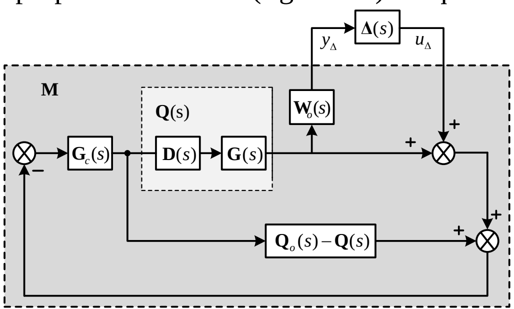

Figure 4.4. M-Δ structure of the proposed controller

Matrix **M** is calculated as follow:

$$\mathbf{M}(s) = -\mathbf{W}_o(s)\mathbf{Q}(s)\mathbf{G}_c(s)\left[\mathbf{I} + \mathbf{Q}_o(s)\mathbf{G}_c(s)\right]^{-1} \quad (4.13)$$

According to the theorem in section 3.2.2, the condition to ensure robust stability with multiplicative output uncertainty is as follow:

$$\mu\left[\mathbf{M}(j\omega)\right] = \mu\left\{\mathbf{W}_o(j\omega)\mathbf{Q}(j\omega)\mathbf{G}_c(j\omega)\left[\mathbf{I} + \mathbf{Q}_o(j\omega)\mathbf{G}_c(j\omega)\right]^{-1}\right\} < 1, \forall\omega \quad (4.14)$$

4.3.2. Design PI/PID controllers for high-order multivariable processes using multi-objective optimization

4.3.2.1. Multi-objective particle swarm optimization (MOPSO)

MOPSO algorithm is described in form of pseudo-code as figure 4.5:

```
A = Ø
for i = 1: N_particle
    initialize x_i, v_i
    constraint(x_i)
    x_Pbest,i = x_i
end
A = dominance(x_Pbest)
k = 0
while k ≤ MAX
    for i = 1: N_particle
        v_i(k+1) = ωv_i(k) + c_1ω_1(x_Pbest − x_i(k)) + c_2ω_2(x_Gbest − x_i(k))
        x_i(k+1) = x_i(k) + v_i(k+1)
        constraint(x_i)
        x_i = mutate(x_i)
        if x_i domninates x_Pbest,i
            x_Pbest,i = x_i
        end
    end
    A = dominance(x_Pbest)
    update (A)
    k = k+1
end
```

Figure 4.5. The pseudo code of MOPSO algorithm

4.3.2.2. Using MOPSO to design a general-oder PI controller.

Consider a closed-loop control system as shown in Figure 4.6, where g_c is the proposed controller; q is the diagonal component of the decoupled matrix; r, d are the setpoint and disturbance signal respectively

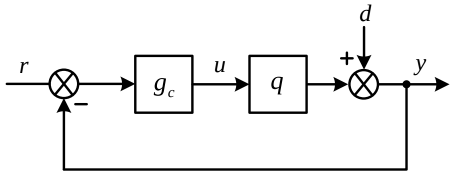

Figure 4.6 The classical closed loop systems

The controller in this case is derived from the proposed controller (4.12) without using the filter ($\tau_F = 0$), and is rewritten as follows:

$$g_c(s) = \frac{1}{s^{\sigma}}\left(K_c + \frac{K_I}{s^{\lambda}}\right) \tag{4.15}$$

The controller is designed to achieve a compromise between system response and disturbance resistance, so a multi-objective optimization algorithm is used. The design steps are as follows:

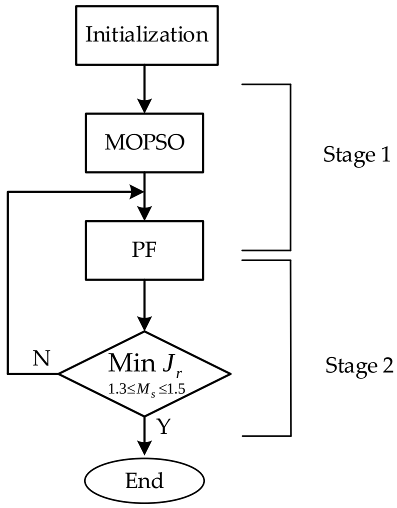

Figure 4.7 The flowchart of the proposed tuning steps

Stage 1: using MOPSO algorithm:

Min $\boldsymbol{J}(\boldsymbol{x}) = \left[\boldsymbol{J}_r(\boldsymbol{x}), \boldsymbol{J}_d(\boldsymbol{x})\right]$

where, $\boldsymbol{x} = \left[K_c \quad K_I \quad \lambda \quad \sigma\right]^T$; $\boldsymbol{J}_r, \boldsymbol{J}_d$ are IAE indices, Eq. (3.1)

$$\text{The constraints: } \begin{cases} K_{c\min} < K_c < K_{c\max} \\ 0 < K_I < K_{I\max} \\ 0.7 \le \lambda \le 1 \\ 0 \le \sigma \le 0.3 \end{cases} \tag{4.16}$$

where, $\lambda \in [0.7,\ 1]$, $\left(\sigma \in [0, 0.3]\right)$ and $K_{c\min}$, $K_{c\max}$, $K_{I\max}$ are chosen based on open loop response of the system.

Stage 2: After obtaining the PF from stage 1, the maximum sensitivity function (3.4) is suggested to appropriately choose the control paramters to guarantee the robust stability of each control loop

$$M_s \triangleq \max_{\omega \in [\omega_l, \omega_h]} \left| \frac{1}{1 + g_c(s) q(s)} \right|_{s = j\omega} \tag{4.17}$$

4.3.2.3 Robust stability analysis of the multivariable processes.

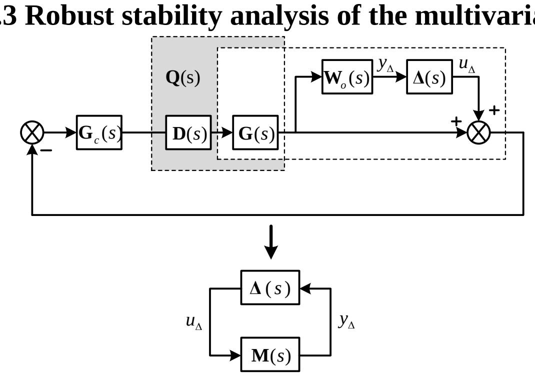

Figure 4.8. **M-Δ** structure for robust stability analysis

In figure 4.8, matrix $\mathbf{M}(s)$ is calculated as follow:

$$\mathbf{M}(s) = -\mathbf{W}_o(s)\mathbf{Q}(s)\mathbf{G}_c(s)\left[\mathbf{I} + \mathbf{Q}(s)\mathbf{G}_c(s)\right]^{-1} \tag{4.18}$$

According to the theorem in section 3.2.2, the condition to ensure robust stability with multiplicative output uncertainty is as follow:

$$\mu\left[\mathbf{M}(j\omega)\right] = \mu\left\{\mathbf{W}_o j\omega)\mathbf{Q}(j\omega)\mathbf{G}_c(j\omega)\left[\mathbf{I} + \mathbf{Q}(j\omega)\mathbf{G}_c(j\omega)\right]^{-1}\right\} < 1, \quad \forall \omega \tag{4.19}$$

Chapter 5. SIMULATION AND EXPERIMENT

5.1 Simulation study

To ensure objectivity when simulating and verifying the proposed methods, and to easily compare with other famous methods, benchmark models commonly used in the field of process control are considered to evaluate the control responses as well as the robustness of the proposed methods.

5.1.1. The proposed method for TITO processes

5.1.1.1 Distillation column Vinante and Luyben (VL)

Transfer function matrix of VL column was first introduced by Luyben [143], the matrix is as follow:

$$\mathbf{G}(s)=\begin{bmatrix}\dfrac{-2.2e^{-s}}{7s+1} & \dfrac{1.3e^{-0.3s}}{7s+1}\\ \dfrac{-2.8e^{-1.8s}}{9.5s+1} & \dfrac{4.3e^{-0.35s}}{9.2s+1}\end{bmatrix}$$

The decoupling matrix is obtained:

$$\mathbf{D}(s)=\begin{bmatrix}1 & 0.591\\ \dfrac{0.651(9.2s+1)e^{-1.45s}}{9.5s+1} & 1\end{bmatrix} \quad (5.1)$$

The two diagonal components of the decoupled matrix can be calculated according to table 4.2 (in the thesis) as follows:

$$q_{11}=g_{11}-\frac{g_{12}g_{21}}{g_{22}}=\frac{-2.2e^{-s}}{7s+1}+\left(\frac{1.3e^{-0.3s}}{7s+1}\right)\left(\frac{2.8e^{-1.8s}}{9.5s+1}\right)\left(\frac{9.2s+1}{4.3e^{-0.35s}}\right) \quad (5.2)$$

$$q_{22}=g_{22}-\frac{g_{12}g_{21}}{g_{11}}=\frac{4.3e^{-0.35s}}{9.2s+1}-\left(\frac{1.3e^{-0.3s}}{7s+1}\right)\left(\frac{2.8e^{-1.8s}}{9.5s+1}\right)\left(\frac{7s+1}{2.2e^{-s}}\right) \quad (5.3)$$

The PSO algorithm will be used to approximate two complex transfer functions q_{11} and q_{22}, the approximate results are:

$$\bar{q}_{11}=\frac{-1.3629e^{-s}}{6.6757s^{0.97}+1};\qquad \bar{q}_{22}=\frac{2.6679e^{-0.3s}}{8.8871s^{0.9683}+1} \quad (5.4)$$

The step response of the original transfer functions and the corresponding approximate functions are compared in figures 5.1 and 5.2. The approximate responses are also compared with the coefficient matching (CM) method proposed by Vu and Lee [67]. In this case, the results are equivalent and almost equivalent to the responses of the original transfer functions

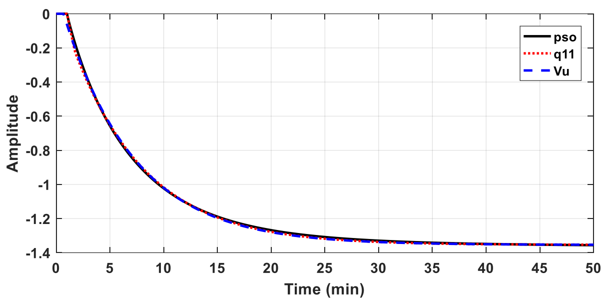

Figure 5.1.Step responses of q_{11} and its approximation (VL)

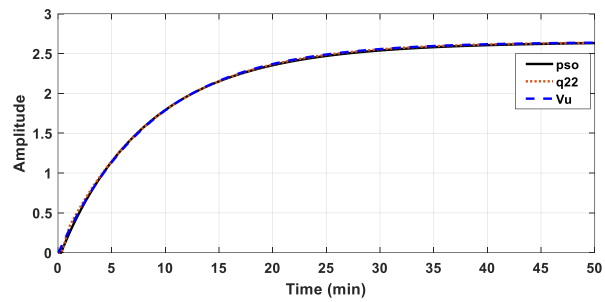

Figure 5.2.Step responses of q_{22} and its approximation (VL)

Based on Table 4.3 in the thesis, in this case, the desired response time constants for the two control loops are chosen $\tau_c=1.9$ and $\tau_c=1.6$, respectively. Two FOPI controllers for two control loops have the following form:

$$g_{c1}(s)=-2.5765\frac{1}{s^{0.03}}\left(1+\frac{1}{6.6757s^{0.97}}\right)\qquad g_{c2}(s)=2.082\frac{1}{s^{0.0317}}\left(1+\frac{1}{8.8871s^{0.9683}}\right) \quad (5.5)$$

Simulation results of the proposed algorithm and comparison with other methods: simplified decoupling combining Smith predictor with integer-order controller (SDSP [144]) and centralized inverted decoupling (Garrido [68]) and are presented in Figure 5.3a, b. Figure 5.4 demonstrates the robust stability of the proposed controller. Table 5.1 summarizes performance indices.

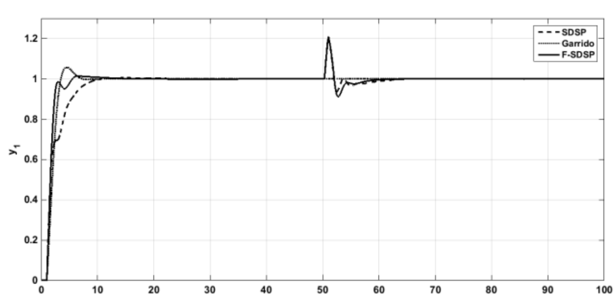

Figure 5.3a. Step responses of control loop 1 (VL)

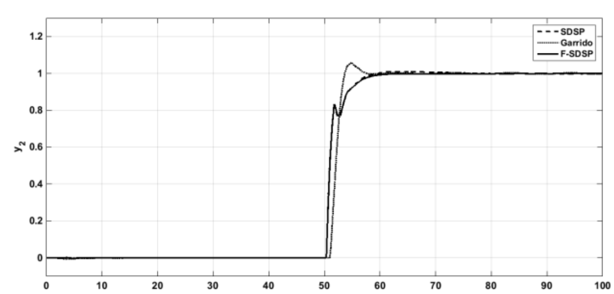

Figure 5.3b. Step responses of control loop 2 (VL)

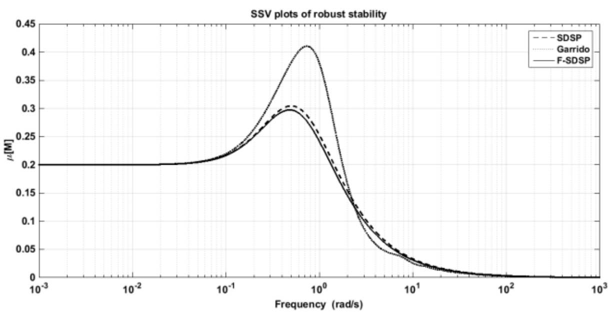

Figure 5.4. SSV plots for robust stability (VL)

Table 5.1. Performance indices of VL column

Methods	IAE	ITAE	TV	$\mu[\mathbf{M}]$
Proposed (F-SDSP)	3.7490	101.66	10.838	0.2974
SDSP	3.4382	102.83	8.7549	0.3046
Garrido	4.5255	126.04	11.295	0.4107

5.1.1.2 Heavy oil fractionator

The heavy oil fractionator is a 2×2 process often used to study control algorithms of multivariable systems in the field of process control [70,145]. Its transfer function matrix has the following equation

Decoupling matrix is obtained:

$$\mathbf{G}(s)=\begin{bmatrix}\dfrac{4.05e^{-27s}}{27s+1} & \dfrac{1.77e^{-28s}}{60s+1}\\ \dfrac{5.39e^{-18s}}{50s+1} & \dfrac{5.72e^{-14s}}{60s+1}\end{bmatrix} \qquad \mathbf{D}(s)=\begin{bmatrix}1 & -\dfrac{0.437(27s+1)e^{-s}}{60s+1}\\ -\dfrac{0.9423(60s+1)e^{-4s}}{50s+1} & 1\end{bmatrix} \tag{5.6}$$

To design a controller for each feedback loop of the system, the diagonal components of the decoupled matrix must be calculated. Based on the formulas in table 4.2 of the thesis, we can calculate as follows

$$q_{11}=g_{11}-\frac{g_{12}g_{21}}{g_{22}}=\frac{4.05e^{-27s}}{27s+1}-\left(\frac{1.77e^{-28s}}{60s+1}\right)\left(\frac{3.39e^{-18s}}{50s+1}\right)\left(\frac{60s+1}{5.72e^{-14s}}\right) \tag{5.7}$$

$$q_{22}=g_{22}-\frac{g_{12}g_{21}}{g_{11}}=\frac{5.72e^{-14s}}{60s+1}-\left(\frac{1.77e^{-28s}}{60s+1}\right)\left(\frac{5.39e^{-18s}}{50s+1}\right)\left(\frac{27s+1}{4.05e^{-27s}}\right) \tag{5.8}$$

Using the PSO algorithm to approximate the above two transfer functions, the results are as follows:

$$\overline{q}_{11}(s)=\frac{2.3979e^{-27s}}{15.1333s^{1.1334}+6.9815s+1};\quad \overline{q}_{22}(s)=\frac{3.3877e^{-14s}}{45.6092s^{0.9967}+1} \tag{5.9}$$

Figures 5.5 and 5.6 illustrate the step responses of the original transfer functions compared to the approximated transfer functions. It can be seen that using the PSO algorithm gives quite good approximation results, for example in the case of the response of loop 2, the response of the original function and the approximated function almost the same.

In this case the desired response time constants for the two loops are chosen $\tau_c=14$ and $\tau_c=20$, respectively. Two FOPI controllers for two control loops have the following form

$$g_{c1}(s)=0.0622\left(1+\frac{1}{4.166s}+5.7077s^{0.1759}\right)\frac{1}{7s+1};\qquad g_{c2}(s)=\frac{0.6732}{s^{0.0033}}\left(1+\frac{1}{45.6092s^{0.9967}}\right) \tag{5.10}$$

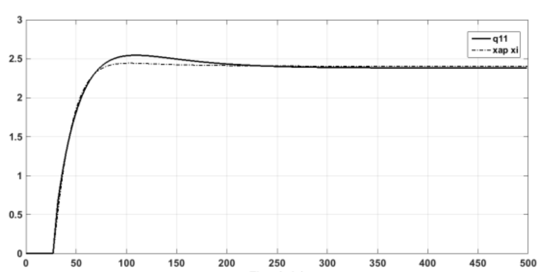

Figure 5.5. Step responses of q_{11} its approximation (heavy oil)

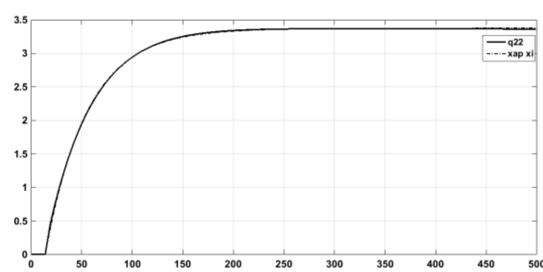

Figure 5.6.Step responses of q_{22} and its approximation (heavy oil)

The simulation results of the proposed method are shown in Figures 5.7 a, b. Furthermore, to increase convincingness, the response is also compared with other methods such as: inverted decoupling combined internal model control with filter (IDIMC-F), and centralized inverted decoupling (ID-K) was proposed by Garrido [70]

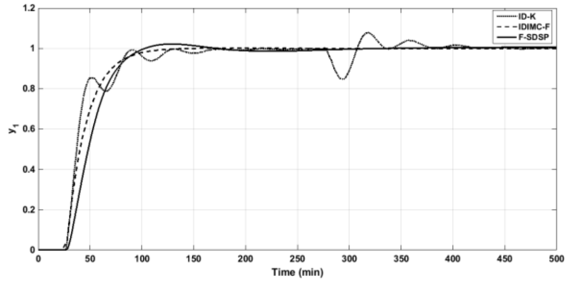

Figure 5.7 a. Step responses of control loop 1 (heavy oil)

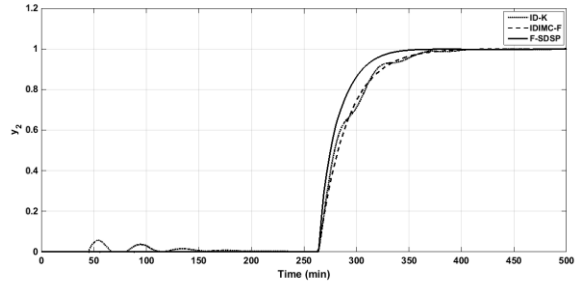

Figure 5.7 b. Step responses of control loop 2 (heavy oil)

Parameters on performance and robustness indices are listed in table 5.2. In addition, Figure 5.8 illustrates the SSV plots to evaluate the robust stability of the proposed controller compared to other methods.

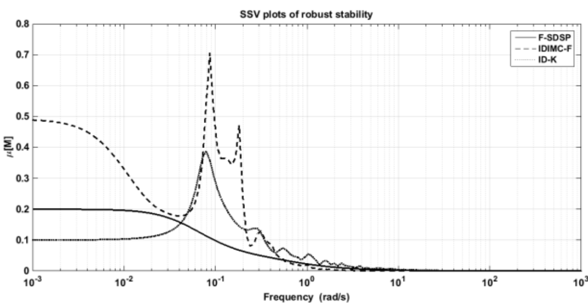

Hình 5.8. The SSV plots for robust stability

Table 5.2. Performance indices of the heavy oil fractionator

Methods	IAE	ITAE	TV	$\mu[\mathbf{M}]$
Proposed (F-SDSP)	57.824	10173	1.4838	0.200
IDIMC-F	750.00	218750	1.7289	0.7068
ID-K	95.521	14561	14.678	0.3880

5.1.2. The proposed method for high-order multivariable processes

5.1.2.1 Ogunnaike and Ray (OR) distillation column

The well-known OR distillation column used to separate mixtures of ethanol and water is widely used in simulation studies in the field of process control [55, 67-69]. Open-loop transfer function matrix and decoupling matrix:

$$\mathbf{G}(s)=\begin{bmatrix} \dfrac{0.66e^{-2.6s}}{6.7s+1} & \dfrac{-0.61e^{-3.5s}}{8.64s+1} & \dfrac{-0.0049e^{-s}}{9.06s+1} \\ \dfrac{1.11e^{-6.5s}}{3.25s+1} & \dfrac{-2.36e^{-3s}}{5s+1} & \dfrac{-0.01e^{-1.2s}}{7.09s+1} \\ \dfrac{-34.68e^{-9.2s}}{8.15s+1} & \dfrac{46.2e^{-9.4s}}{10.9s+1} & \dfrac{0.87(11.61s+1)e^{-s}}{(3.89s+1)(18.8s+1)} \end{bmatrix} \quad \mathbf{D}(s)=\begin{bmatrix} 1 & 0.7549\dfrac{(0.8337s+1)}{0.533s+1}e^{-0.9s} & 0.0062e^{-0.5233s} \\ 0.3905e^{-2.71s} & 1 & -0.0014 \\ 19.8247\dfrac{(13.8874s+1)}{8.7956s+1}e^{-8.2s} & -23.1741\dfrac{(2.0113s+1)}{5.5621s+1}e^{-8.4s} & 1 \end{bmatrix} \tag{5.11}$$

The diagonal components of the decoupled matrix can be calculated as follows:

$$\bar{q}_{11}=\frac{0.3298(23.1802s+1)e^{-2.6s}}{(21.1355s+1)(3.7363s+1)};\ \bar{q}_{22}=\frac{-1.2973e^{-3s}}{(1.2739s+1)(0.5014s+1)};\ \bar{q}_{33}=\frac{0.5601(17.4859s+1)e^{-s}}{(20s+1)(2.6915s+1)} \tag{5.12}$$

The design sequence includes 2 steps: the first step will be to find the PF containing feasible solutions of the multi-objective optimization problem, and then select the most appropriate solution based on performance criteria and robustness index M_s. Figure 5.9 a, b, and c illustrate the results of the PF achieved by each control loop, the set of feasible solutions of the optimization problem converges to the Pareto front. The final control parameters achieved are summarized in table 5.3.

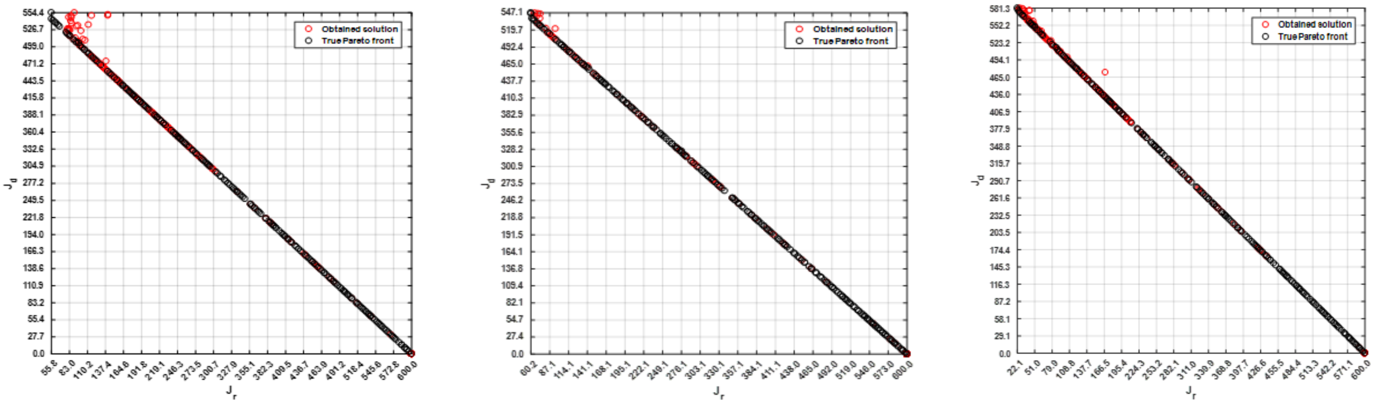

Figure 5.9 a, b, and c. The obtained PFs using two objective functions J_r and J_d

In this example, the proposed method is compared with methods such as multi-loop PI/PID controller [55] and centralized PI controller (CPI) [146]. The simulation results are shown in Figures 5.10 a, b, and c. Similar to the previous example, the criterion μ is used to evaluate the robustness of the proposed method. The weight matrix for the output multiplicative uncertainty of the three diagonal components of the decoupled matrix is selected as follows:

$$\mathbf{W}_{\mathrm{o}}(s) = \mathrm{diag}\left\{-\frac{s+0.2}{0.5s+1},\quad -\frac{s+0.2}{0.5s+1},\quad -\frac{s+0.2}{0.5s+1}\right\} \tag{5.13}$$

This weight matrix corresponds to approximately 20% of the error of the gain parameter. Figure 5.11 demonstrates that the structured singular value (SSV) of the proposed method always ensures the stability of the control system. Meanwhile, in other methods, the value of μ has a peak exceeding 1, meaning the control system will be unstable in this case.

Table 5.3. Control parameters and performance indices of OR column.

Phương pháp	Vòng	K_{ci}	K_{Ii}	τ_{Di}	λ_i	σ_i	$\mu[\mathbf{M}]$	IAE	TV
Đề xuất	1	1.504	0.157	__	1	0.055	0.1002	27.79	4.9783
	2	-0.089	0.970	__	0.832	0.174			
	3	1.377	0.107	__	1	0.01			
Multi-loop	1	2.250	0.140	2.58	__	__	0.2479	39.99	6.1432
	2	-0.490	0.155	3.37	__	__			
	3	4.830	0.322	10.16	__	__			
CPI	_				__	__			
	_		$^*\mathbf{G}_c(s)$		__	__	0.1276	25.73	4.9336

***G**$_c(s)$: full matrix (3×3), it means that we need 9 PI controllers, detail matrix can be refered in [146]

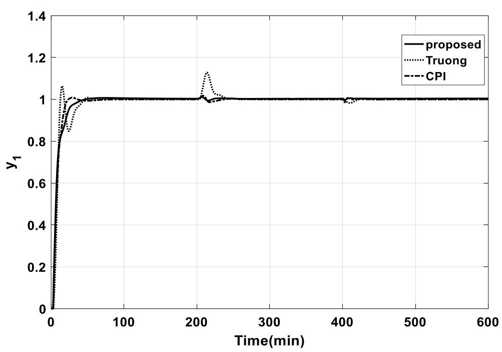

Figure 5.10 a. Step responses of control loop 1 (OR)

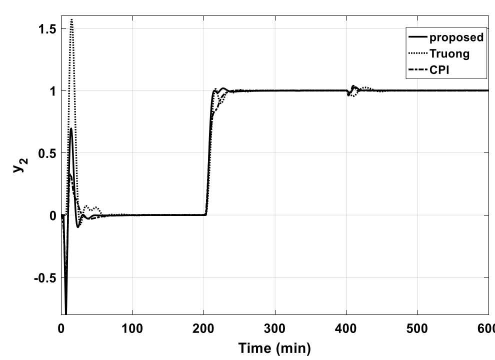

Hình 5.10 b. Step responses of control loop 2 (OR)

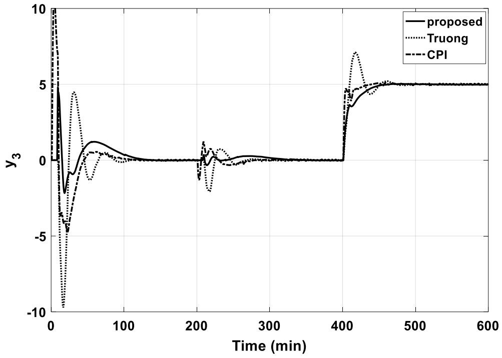

Figure 5.10 c. Step responses of control loop 3 (OR)

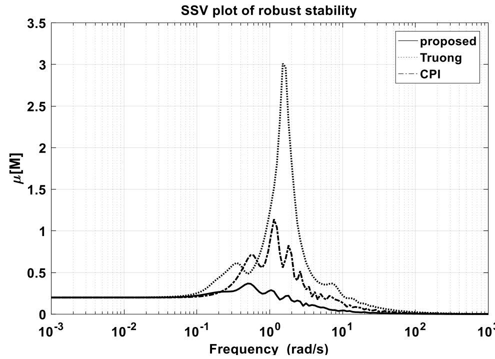

Figure 5.11. The SSV plots for robust stability (OR)

5.1.2.2. HVAC for temperature control (4×4)

The temperature control model for four connected rooms is known as the HVAC process [64]. The transfer function matrix represents the process represented by a (4×4) matrix (5.14)

$$\mathbf{G}(s)=\begin{bmatrix}\frac{-0.098e^{-17s}}{122s+1} & \frac{-0.036e^{-27s}}{149s+1} & \frac{-0.014e^{-32s}}{158s+1} & \frac{-0.017e^{-30s}}{155s+1}\\ \frac{-0.043e^{-25s}}{147s+1} & \frac{-0.092e^{-16s}}{130s+1} & \frac{-0.011e^{-33s}}{156s+1} & \frac{-0.012e^{-34s}}{157s+1}\\ \frac{-0.012e^{-31s}}{153s+1} & \frac{-0.016e^{-34s}}{151s+1} & \frac{-0.102e^{-16s}}{118s+1} & \frac{-0.033e^{-26s}}{146s+1}\\ \frac{-0.013e^{-32s}}{156s+1} & \frac{-0.015e^{-31s}}{159s+1} & \frac{-0.029e^{-25s}}{144s+1} & \frac{-0108e^{-18s}}{128s+1}\end{bmatrix} \tag{5.14}$$

The decoupling matrix [67, 144]:

$$\mathbf{D}(s)=\begin{bmatrix}1 & \frac{-0.341(121.918s+1)e^{-9.151s}}{146.753s+1} & \frac{-0.081(132.251s+1)e^{-11.943s}}{164.976s+1} & \frac{-0.115(124.604s+1)e^{-8.887s}}{147.929s+1}\\ \frac{-0.457(130.872s+1)e^{-8.77s}}{147.641s+1} & 1 & \frac{-0.049(235.202s+1)e^{-12.986s}}{228.983s+1} & \frac{-0.04(188.514s+1)e^{-14.432s}}{170.865s+1}\\ \frac{-0.03(187.93s+1)}{175s+1} & \frac{-0.093(97.617s+1)e^{-15.187s}}{117.144s+1} & 1 & \frac{-0.304(118.386s+1)e^{-9.165s}}{145.037s+1}\\ \frac{-0.049(1946.796s+1)e^{-11.409s}}{1946.775s+1} & \frac{-0.073(152.319s+1)e^{-6.741s}}{166.805s+1} & \frac{-0.252(124.823s+1)e^{-6.104s}}{138.501s+1} & 1\end{bmatrix} \tag{5.15}$$

Using PSO algorithm to approximate the transfer functions, the diagonal elements of decoupled matrix are as follows:

$$q_{11}=\frac{-0.0804e^{-17s}}{109.0896s+1};\ q_{22}=\frac{-0.0736e^{-16s}}{117.2055s+1};\ q_{33}=\frac{-0.092e^{-16s}}{112.2966s+1};\ q_{44}=\frac{-0.097e^{-18s}}{121.0125s+1} \tag{5.16}$$

In this example, the centralized PI controller (CPI) method proposed by Ghosh and Pan [146] and the optimal retuning method (1-ODP) proposed by Khandelwall and Detroja [147] are selected to compare with the proposed method. Similar to the previous example, after using the proposed method, the controller parameters are achieved as shown in table 5.4. From this table, we see that the integral term of the controller always has integer order in this case, meaning that the optimal controller for the HVAC system is the traditional PI controller.

Table 5.4. Control parameters and performance indices of HVAC

Methods	Loop	K_{ci}	K_{Ii}	λ_i	σ_i	$\mu[\mathbf{M}]$	IAE	TV
Proposed	1	-23.799	0.0094	1	__	0.2019	199.72	207.146
	2	-37.292	0.0091	1	__			
	3	-28.036	0.0099	1	__			
	4	-26.882	0.0085	1	__			
					__			

1-ODP	_	$G_{c-1ODP}(s)^{*}$	_	—	0.2287	372.03	340.492
CPI	_	$G_{c-CPI}(s)^{**}$	_	—	0.1999	376.60	200.588

*****G$_{c\text{-}1ODP}$(s) và ******G$_{c\text{-}CPI}$(s): are full matrix (4×4), it means that we need 16 controllers, detail matrices can be refered to [146]

In this section, the sequential change of the set-point is performed at times t = 0 (min), t = 500 (min), t = 1000 (min), and t = 1500 (min) respectively for control loops 1 to 4. Figure 5.12 a, b, c and d illustrates the response of the proposed controller and other controllers when the set-point and disturbance change.

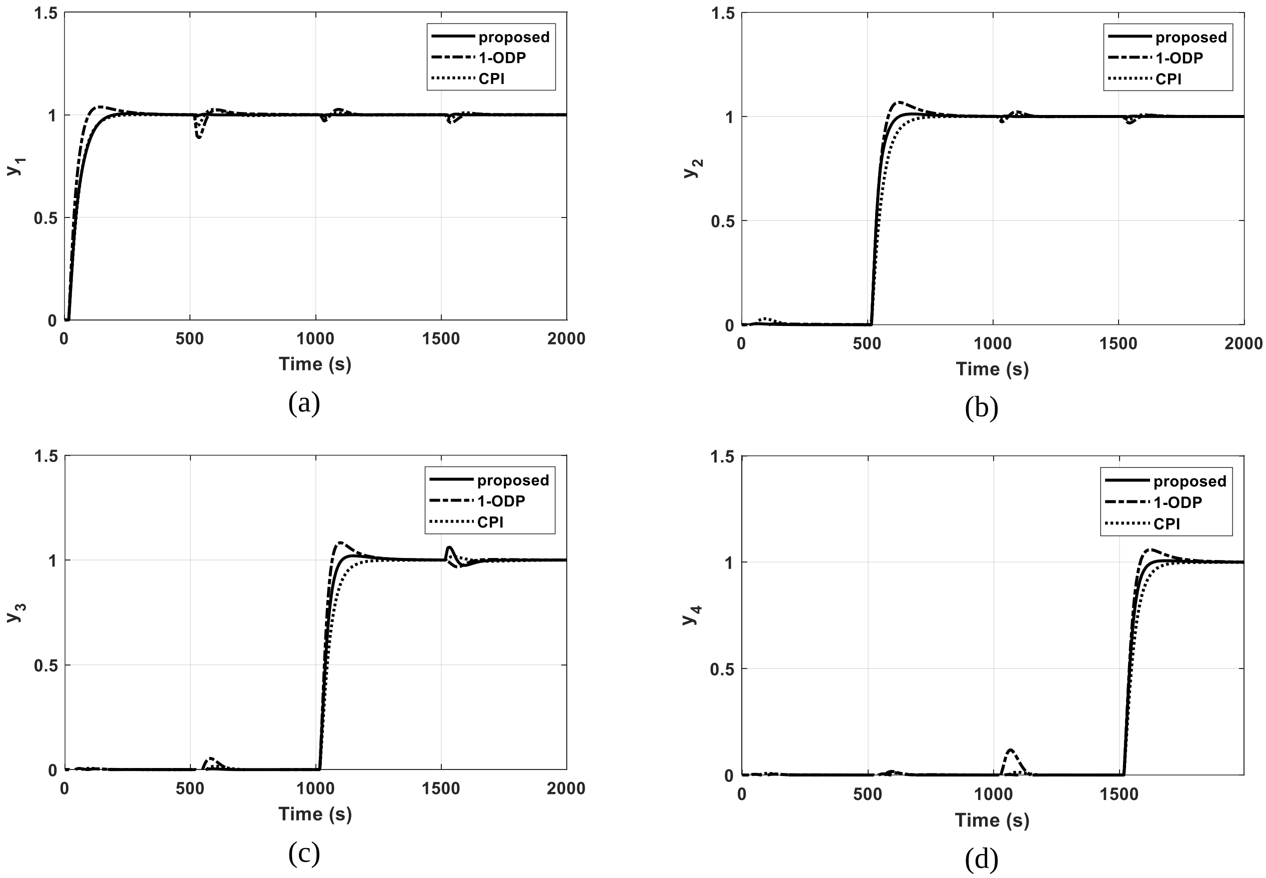

Figure 5.12 a, b, c and d. Step responses of 4 control loops respectively

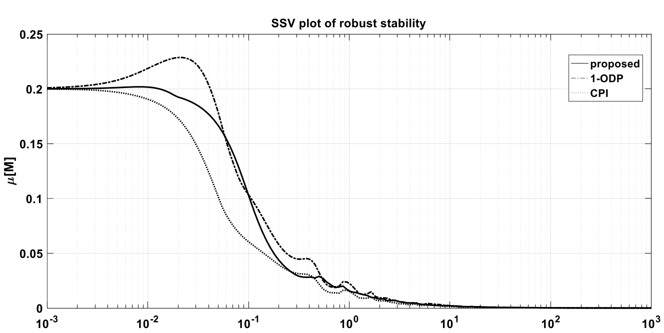

Figure 5.13 shows the plots of μ all three methods and all ensure robust stability in the presence of uncertainty signals with a multiplicative output error.

Figure 5.13 The SSV plots for robust stability of HVAC

5.2 Experiment on fractional-order control for multivariable systems

To verify the applicability of the proposed controller as well as the performance of the fractional-order controller for multivariable systems, in this thesis, the author experiments on a system of quadruple tank.

5.2.1 Introduction to the experimental model

Figure 5.15 is the quadruple-tank system used for experiment. The flow of liquid pumped into the tanks is controlled by two AC centrifugal pumps with pump speed adjusted by two inverters with control voltages u_1, u_2 (0–10 VDC). Two three-way valves V_1 and V_2 divide the flow out of the pump into the upper and lower tanks (crossing each other as the figure) with two dividing factors γ_1 and γ_2 ($0<\gamma_1,\gamma_2<1$). The liquid levels in the two lower tanks are h_1, h_2 (m) and are measured by 2 capacitive sensors (LT_1, LT_2) with the output signal being the industrial standard current (4-20 mA) corresponding to the liquid level (0 – 0.6 m); Using a current-voltage converter to convert current into a voltage of 0-5 VDC. Four tanks have rectangular cross-sections areas A_1, A_2, A_3 and A_4 (m^2) respectively.

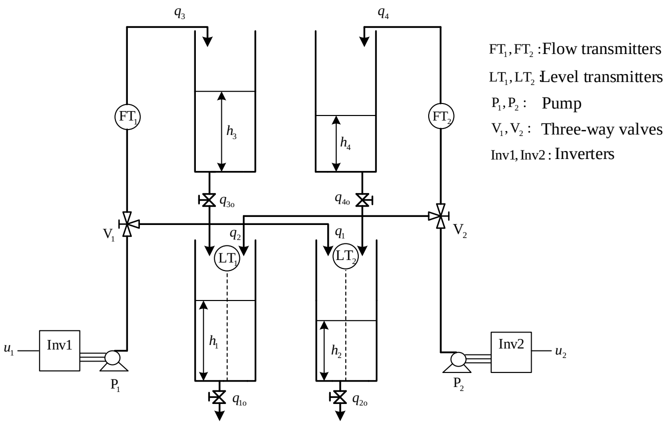

Figure 5.14. Diagram of the quadruple tank system

The matrix transfer function of the system:

$$\begin{bmatrix} X_1(s) \\ X_2(s) \end{bmatrix} = \begin{bmatrix} \dfrac{K_1(1-\gamma_1)}{(\tau_1 s+1)(\tau_3 s+1)} & \dfrac{K_2\gamma_2}{\tau_1 s+1} \\ \dfrac{K_3\gamma_1}{\tau_2 s+1} & \dfrac{K_4(1-\gamma_2)}{(\tau_2 s+1)(\tau_4 s+1)} \end{bmatrix} \begin{bmatrix} R_1(s) \\ R_2(s) \end{bmatrix} \tag{5.17}$$

$$\text{where: } K_1=\frac{\tau_1 k_1}{A_1};\ K_2=\frac{\tau_1 k_2}{A_1};\ K_3=\frac{\tau_2 k_1}{A_2};\ K_4=\frac{\tau_2 k_2}{A_2} \tag{5.18}$$

Figure 5.15 (a) The quadruple tank system

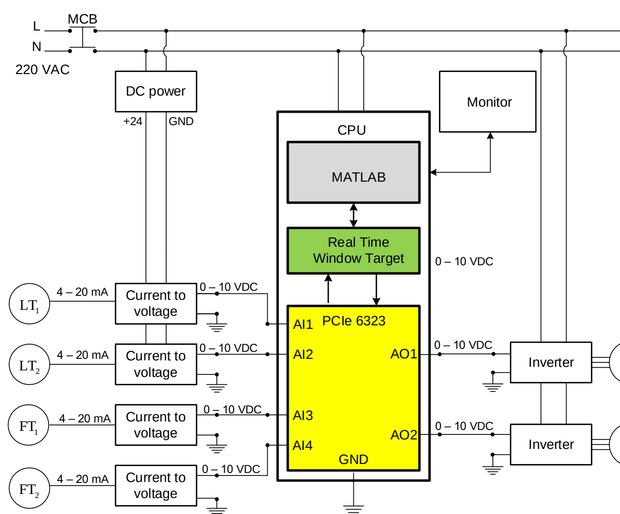

(b) Block diagram of the controller

The quadruple tank system is a 2×2 process with input signals being two pump control voltages and two outputs being the liquid level in the two lower tanks. This system is chosen for many academic simulation or experiment in the field of process control because the dynamic characteristics of the system will change differently depending on the coefficient γ_1,γ_2. Figure 5.15 (a) is the actual system including the water tanks and control cabinet. Figure 5.15 (b) is a diagram of the data acquisition (DAQ PCIe 6323) and other hardware devices used in the system.

5.2.2 System identification using the proposed method

According to the system identificaton theory presented in chapter 2, the author conducted experiments to find the mathematical model for the system.

5.2.2.1 Data acquisition

Although the dynamic of the system is nonlinear, after approximating around the operating point, the system can be represented in linear form with a 2×2 transfer function matrix, equation (5.17). Therefore, in this case, we choose the input signal as a pseudo random binary signal (PRBS).

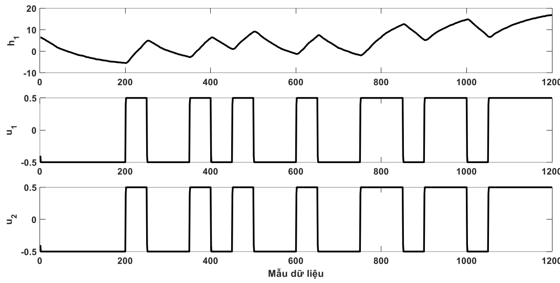

Figure 5.16. In-out data for loop 1 identification

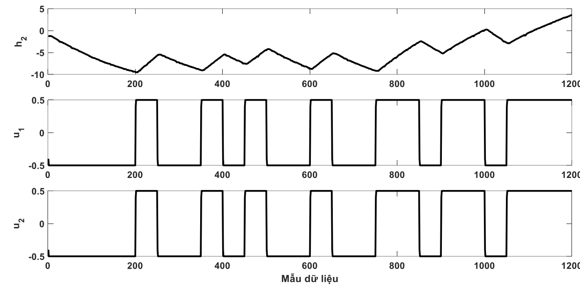

Figure 5.17. In-out data for loop 2 identification

5.2.2.2. Using LS method for the two-input, two-output (TITO) system

Eq. 5.17 can be represented by a general matrix as follows:

$$\begin{bmatrix} y_1(t) \\ y_2(t) \end{bmatrix} = \begin{bmatrix} G_{11}(q) & G_{12}(q) \\ G_{21}(q) & G_{22}(q) \end{bmatrix} \begin{bmatrix} r_1(t) \\ r_2(t) \end{bmatrix} + \begin{bmatrix} v_1(t) \\ v_2(t) \end{bmatrix} \tag{5.19}$$

Applying the LS method mentioned in section 3.2 to each output, assuming the first output (the other is completely similar), we have

$$V_{LS1} = \frac{1}{N} \sum_{k=n_1+1}^{N} \left[A_{11}(q) y_1(k) - \left(B_{11}(q) r_1(k) + B_{12}(q) r_2(k) \right) \right]^2 \tag{5.20}$$

Solutions of (5.20) are obtained from Eq. (2.15), where:

- n_1, n_2, n_3 are orders of $A_{11}(q)$, $B_{11}(q)$, $B_{12}(q)$ ($n_1 > n_2 > n_3$)
- $\mathbf{y} = \begin{bmatrix} y_1(n_1+1) \\ y_1(n_1+2) \\ \vdots \\ y(N) \end{bmatrix}$; $\boldsymbol{\theta} = \left[a_{11,1} \dots a_{11,n_1} \ b_{11,1} \dots b_{11,n_2} \ b_{12,1} \dots b_{12,n_3} \right]^T$
- $\boldsymbol{\varphi} = \begin{bmatrix} -y_1(n_1) & \dots & -y_1(1) & r_1(n_1) & \dots & r_1(1) & r_2(n_1) & \dots & r_2(1) \\ \vdots & \ddots & \vdots & \vdots & \ddots & \vdots & \vdots & \ddots & \vdots \\ -y_1(N-1) & \dots & -y_1(N-n_1) & r_1(N-1) & \dots & r_1(N-n_1) & r_2(N-1) & \dots & r_2(N-n_1) \end{bmatrix}$

5.2.2.3. Validation

Using 800 samples from collected data to validate the identified results :

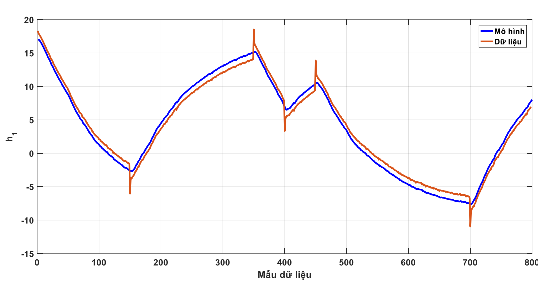

Figure 5.18. Validation of identified parameters of loop 1

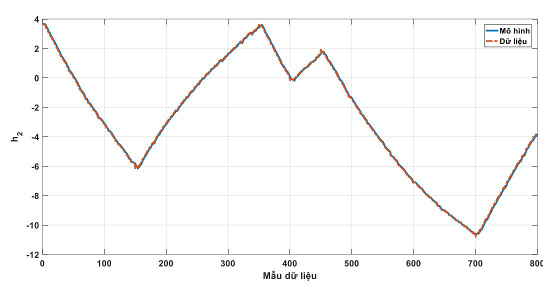

Figure 5.19 Validation of identified parameters of loop 2

Paramerters $\boldsymbol{\theta}$ of both loops are obtained:

$$\boldsymbol{\theta}_1 = \begin{bmatrix} -1.4371 \\ -0.0059 \\ 0.4430 \\ 0.0000 \\ 0.0002 \end{bmatrix} \quad \boldsymbol{\theta}_2 = \begin{bmatrix} -1.4280 \\ 0.0183 \\ 0.4098 \\ 0.0002 \\ 0.0001 \end{bmatrix} \tag{5.21}$$

Converting to continous transfer functions with sample time T_s = 0.1 (s)

$$G_{11}(s) = \frac{0.0002395s^3 + 0.008916s^2 + 0.2691s + 2.807}{s^4 + 15.44s^3 + 1053s^2 + 877.5s + 1.777} \tag{5.22}$$

$$G_{12}(s) = \frac{0.001006s^3 + 0.03744s^2 + 1.13s + 11.79}{s^4 + 15.44s^3 + 1053s^2 + 877.5s + 1.777} \tag{5.23}$$

$$G_{21}(s) = \frac{0.001414s^3 + 0.05352s^2 + 1.618s + 16.96}{s^4 + 16.67s^3 + 1065s^2 + 1232s + 2.388} \tag{5.24}$$

$$G_{22}(s) = \frac{0.0006391s^3 + 0.02419s^2 + 0.7314s + 7.669}{s^4 + 16.67s^3 + 1065s^2 + 1232s + 2.388} \tag{5.25}$$

From the dynamic equations of the system, it can be seen that the component transfer functions are only of order 1 or 2. Therefore, we use the proposed approximation technique, the above transfer functions (5.22) to (5.25) are approximated to

$$\bar{G}_{11}(s) = \frac{1.5825e^{-6.85s}}{496.2227s+1};\ \bar{G}_{12}(s) = \frac{6.6411e^{-5.12s}}{495.2328s+1};\ \bar{G}_{21}(s) = \frac{7.1072e^{-5.18s}}{516.9899s+1};\ \bar{G}_{22}(s) = \frac{3.2158e^{-6.55s}}{517.9853s+1} \tag{5.26}$$

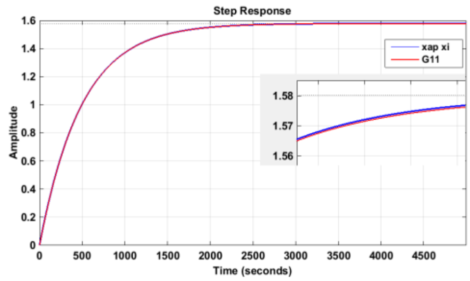

Figure 5.20. Step responses of $G_{11}(s)$ and its approximation

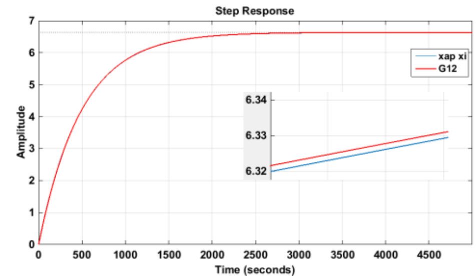

Figure 5.21. Step responses of $G_{12}(s)$ and its approximation

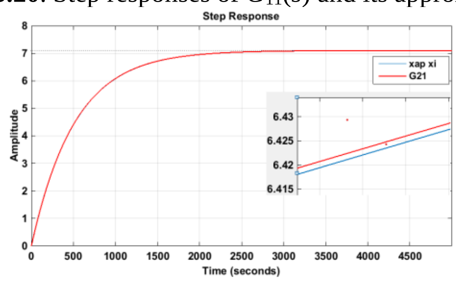

Figure 5.22. Step responses of $G_{21}(s)$ and its approximation

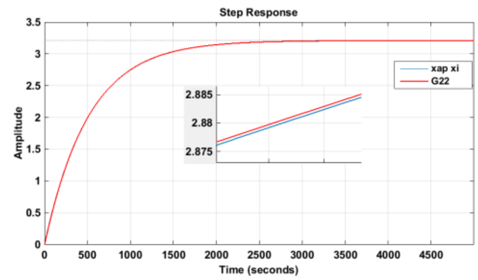

Figure 5.23. Step responses of $G_{22}(s)$ and its approximation

5.2.3 Controller design

Applying the simplified decoupling technique, we can calculate the components of the decoupling matrix as follows

$$d_{12} = -\frac{\bar{G}_{12}}{\bar{G}_{11}} = -\frac{4.1966(496.2227s+1)}{495.2328s+1};\ d_{21} = -\frac{\bar{G}_{21}}{\bar{G}_{22}} = -\frac{2.21(517.9853s+1)}{516.9899s+1} \tag{5.27}$$

According to table 4.2 (2×2), the diagonal components of the decoupled matrix can be calculated as follows

$$q_{11}(s) = \bar{G}_{11} - \frac{\bar{G}_{12}\bar{G}_{21}}{\bar{G}_{22}} = \frac{1.5825e^{-6.85s}}{496.2227s+1} - \frac{\dfrac{6.6411e^{-5.12s}}{495.2328s+1}\dfrac{7.1072e^{-5.18s}}{516.9899s+1}}{\dfrac{3.2158e^{-6.55s}}{517.9853s+1}} \tag{5.28}$$

$$q_{22}(s) = \bar{G}_{22} - \frac{\bar{G}_{12}\bar{G}_{21}}{\bar{G}_{11}} = \frac{3.2158e^{-6.55s}}{517.9853s+1} - \frac{\dfrac{6.6411e^{-5.12s}}{495.2328s+1}\dfrac{7.1072e^{-5.18s}}{516.9899s+1}}{\dfrac{1.5825e^{-6.85s}}{496.2227s+1}} \tag{5.29}$$

The two Eqs. (5.28) and (5.29) are quite complicated and can not be used to design the corresponding controller. Using the proposed method to approximate q_{11} and q_{22} to the a fractional-order transfer function, Eq. (4.9). Figures 5.24 and 5.25 are the step response of the original functions and the approximated ones.

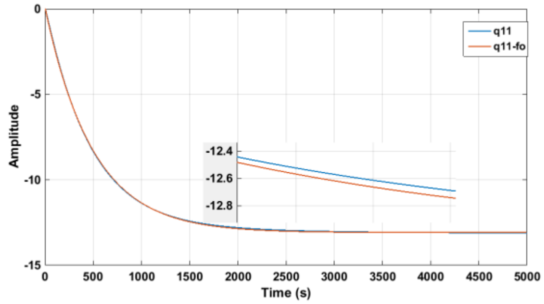

Figure 5.24. Step responses of $q_{11}(s)$ and its approximation

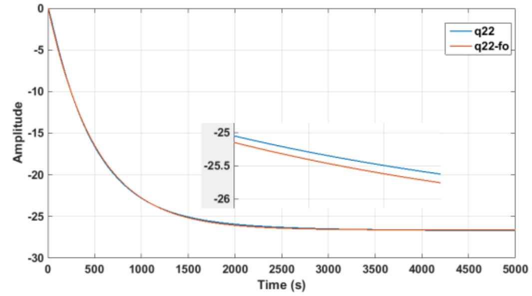

Figure 5.25. Step responses of $q_{22}(s)$ and its approximation

The approximated transfer functions :

$$\bar{q}_{11}(s)=\frac{-13.0755e^{-3.7s}}{219.4076s^{1.2489}+482.2408s+1};\ \bar{q}_{22}(s)=\frac{-26.7e^{-3.45s}}{1209.2s^{1.7}+540.7s+1} \quad (5.30)$$

From the two above transfer functions, equation (5.30), we use the proposed controllers and their design method proposed in chapter 4, the calculation formulas are summarized in table 4.1. The two resulting controllers:

$$g_{c1}(s)=-3.3528\left(1+\frac{1}{482.2408s}+0.455s^{0.2489}\right)\frac{1}{2.5s+1};\ g_{c2}(s)=-2.0251\left(1+\frac{1}{540.7s}+2.2364s^{0.7}\right)\frac{1}{2.5s+1} \quad (5.31)$$

Simulation results of the quadruple tank are shown in Figures 5.26 and 5.27. To evaluate the effectiveness of the proposed method (F-SDSP), the author compared it with other methods: SDSP ([144]) using integer order and inverted decoupling method combined with Smith predictor (SID) (Garrido [80]). The input signals are changed sequentially at the two inputs at times t = 0 and t = 150 (s).

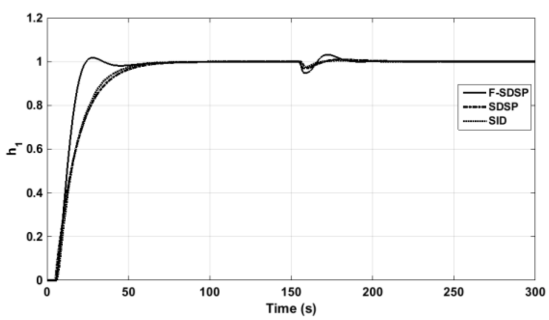

Figure 5.26. Step response of control loop 1

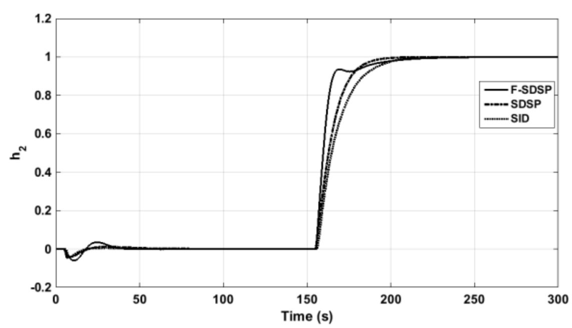

Figure 5.27. Step response of control loop 2

Compared with the SID method, the control signals of the proposed structure (integer and non-integer order) both give better results with significantly smaller TV values (table 5.5). The other performance indices (IAE and ITAE) summarized in table 5.5 also demonstrate that the F-SDSP method gives superior results than the other.

Figure 5.28 evaluates the robust stability of the control system. In this case, the multiplicative output uncertainty with the weight matrix chosen as in simulation problems $\left(\mathbf{W}_0(s)=diag\left\{-\frac{s+0.2}{2s+1},-\frac{s+0.2}{2s+1}\right\}\right)$. In general, in the frequency range (10^{-3} – 10^{3}) rad/s, all methods give similar robust stability. The values μ in table 5.5 also prove that.

Implementing the fractional-order controller according to equations (5.31) together with the simplified decoupler (5.27), using Matlab's Simulink to run in real-time mode (Real-Time Window Target). The controller diagram of the system is built on Simulink as shown in Figure 5.29.

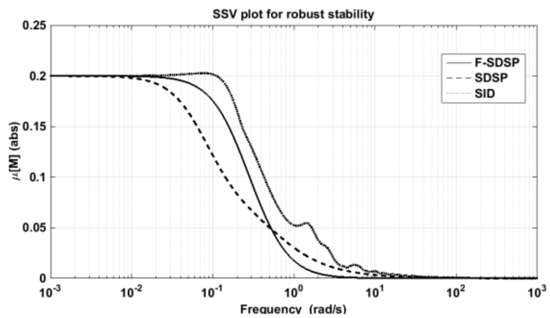

Figure 5.28. The SSV plots for robust stability (quadruple tank)

Bảng 5.5 Performance indices of the quadruple tank system

Method	IAE	ITAE	TV	$\mu[\mathbf{M}]$
F-SDSP	21.2353	1739.5	12.4502	0.2000
SDSP	31.2305	2713.2	5.3683	0.2000
SID	24.9496	2165.3	26.4776	0.2027

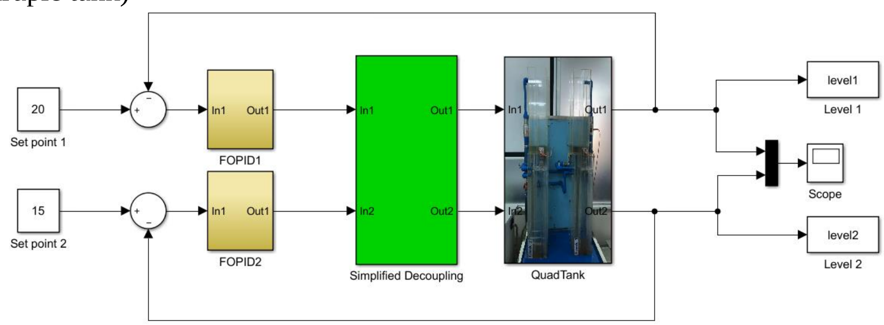

Figure 5.29. Simulink diagram in real-time control mode

The results of controlling the quadruple tank are shown in Figure 5.30 a and b. From the figures, we can see that the control responses of both tanks are similar to the simulation results (Figures 5.26 and 5.27). In tank 1, there is no overshoot and the settling time is about 40 (s); In tank 2, there is an overshoot but not significant and the settling time is about 60 (s). From the responses, we also see that the responses fluctuates slightly, mainly due to sensor noises. The experimental process also proves that the fractional-order controller is capable of controlling real systems.

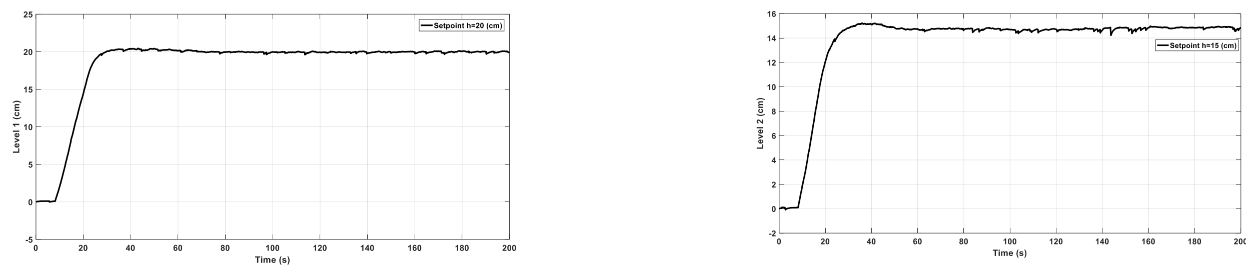

Figure 5.30 a, b. Step responses of levels in both tanks

Figure 5.31 a, b show the control voltages of the system. It can be seen that when the liquid level reaches the desired value (steady state), the control signals change very little with the goal of maintaining the system's set-points. The experimental control signals have low frequency fluctuations due to noises in the measurement signal as well as due to fluctuations in the liquid level in the tank as described above.

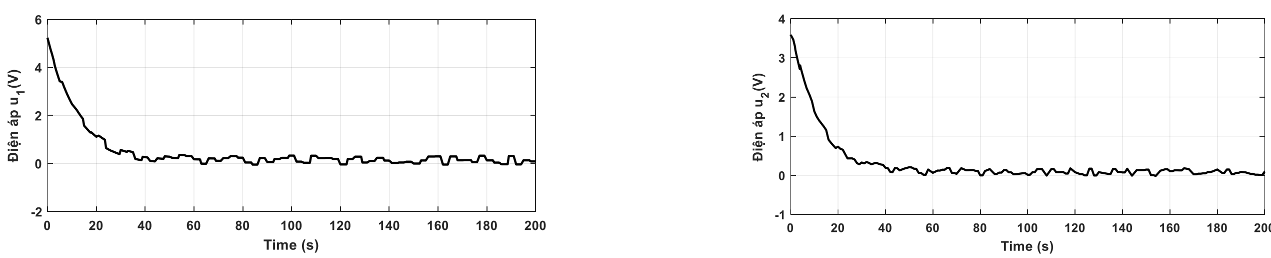

Figure 5.31 a, b. The control voltages in both tanks

Chapter 6. CONCLUSION

6.1 Results

In the thesis, the author focused on research to solve the problems of controlling multivariable processes. The research results are achieved by using fractional-order PID controllers as well as developing the controller structure for multivariable systems. The research results are summarized as follows:

Analyzing the advantages of fractional order in describing the dynamics of some famous equations. From there, the necessity of fractional calculus in the control field is explained. Research the effects of derivatives and integrals of fractional order on control signals in the feedback controller. The simulation results show that the fractional-order controller makes the control signal less affected by noise and also makes the control system more robust.

Proposing a control structure for multivariable systems combining simplified decoupling and the multivariable Smith predictor. The component transfer functions of the decoupling and decoupled matrix are complicated, especially when the degree of the multivariable system increases. In this study, to simplify the above transfer functions to make it easier to design the controller, the author proposes to use the particle swarm optimization (PSO) algorithm to approximate the transfer functions to some simple forms with integer and fractional orders, achieving high accuracy when compared with existing approximation and reduction methods. However, the proposed method is only suitable for linear systems with assumed transfer functions known in advance and can not solve the general problem of any multivariable system. In addition, the multivariable Smith predictor is incorporated into the simplified decoupling structure, which is intended to eliminate the delay times in the characteristic equation of the closed-loop system, leading to a convenient design of the controller.

Based on the proposed structure, the author has also proposed methods to tune fractional-order PI/PID controllers for different multivariable systems. The research is summarized as follows:

- Propose analytical tuning rules for the proposed controller using an internal model control (IMC) for low-order multivariable systems (2×2). The controller parameters are calculated based on the desired response time criterion. However, this method is not general because not all cases can reduce the IMC controller to the form of a fractional order PI/PID controller. For multivariable systems, this method is only suitable for 2×2 systems.
- For high-order systems (3×3 and 4×4), the author proposes a multi-objective particle swarm optimization algorithm (MOPSO) to find the parameters of the controller. The objective function of the optimization problem is to minimize the two steady state errors when the set-point and disturbance change. The feasible solutions of the multi-objective optimization problem will converge to the Pareto front, and from there, the robust stability criterion using the maximum sensitivity function index will be suggested to select the most suitable solution from the Pareto front to ensure the robustness of the control system.

The robustness of the entire control structure will be re-evaluated using the **M-Δ** structure and multiplicative output uncertainty. Normally, this structure is used for integer-order systems, and in this thesis, the author extends it to systems with fractional-order controllers. Simulation results demonstrate the robust stability of the proposed structure and are also better than other control methods and structures.

The experimental quadrature tank (2×2 system) is used to verify the proposed method. First, the identification method for multivariable systems is by using the matrix fraction description (MFD) technique to convert the MIMO system into multiple-input, single-output (MISO) systems. From there, the least squares method of single variable systems is applied to identify system parameters. Then, the proposed method for the 2×2 system is used to design a fractional-order controller and verify it on an experimental system. The controller is designed in Matlab and works well in real-time control mode (Real-Time Window Target).

6.2 Limitations and future works

Besides the achieved results, the research on the project also has many issues that need to be exploited:

- The proposed methods are still not general enough to solve control problems for multivariable systems. Designing a FOPID controller with full tuning rules for all 5 parameters is still a challenging issue for researchers in this field. Furthermore, using explicit design methods for high-order multivariable systems instead of evolutionary algorithms is also an open problem in this field.
- When verifying on the experimental system, the designed controller still runs on Matlab in real-time mode. The complete digital controller implementation of fractional-order control has not been studied in the thesis. And this is also the future work that needs to be focused on developing to bring fractional-order control into applications.
- The experimental system in the thesis can only verify the 2×2 system, higher-order systems such as distillation column processes, due to budget and equipment limitations, have not been implemented in the thesis. This is important applied research to bring control theories into practical applications, and also bringing great economic benefits.

Publications

1. **Chuong, V.L**.; Vu, T.N.L.; Truong, N.T.N.; Jung, J.H. "The Pareto optimal robust design of generalized-order PI Controllers based on the decentralized structure for multivariable processes", *Korean Journal of Chemical Engineering*, 39 (4), pp. 865–975, 2022 (**SCIE, Q2**)
2. Vu, T.N.L., **Chuong, V.L**.; Truong, N.T.N.; Jung, J.H. "Analytical Design of Fractional-Order PI Controller for Parallel Cascade Control Systems", *Appl. Sci.*, 12 (4), 2222, 2022 (**SCIE, Q2**)
3. **Chuong, V.L**.; Vu, T.N.L.; Truong, N.T.N.; Jung, J.H. "A Novel Design of Fractional PI/PID controllers for Two-Input Two-Output Processes", *Appl. Sci*. 2019, *9 (23)*, 5262. (**SCIE, Q1**).
4. **Chuong, V.L**.; Vu, T.N.L.; Truong, N.T.N.; Jung, J.H. "An Analytical Design of Simplified Decoupling Smith Predictors for Multivariable Processes", *Appl. Sci*. 2019, *9 (12)*, 2487. (**SCIE, Q1**).
5. **Vo Lam Chuong**, Truong Nguyen Luan Vu, Le Linh, "Fractional PI control for Coupled-Tank MIMO System", *4th Int. Conf. on Green Technology and Sustainable Development*, **2018.**
6. **Vo Lam Chuong**, Truong Nguyen Luan Vu, "Identification and Dynamic Matrix Control algorithm for a Heating Process", *Int. Conf. on System Science and Engineering, ICSSE*, p. 642-645, **2017**.
7. **Vo Lam Chuong**, Truong Nguyen Luan Vu, "Identification Method for Simplified Decoupling Control of Multivariable Processes", *Journal of Technical Science*, No. 44A, pp.76-82, **2017**.
8. T. N. L. Vu, L. H. Giang, Le Linh**, V. L. Chuong**, "Advanced IMC-PID controller design for the disturbance rejection of first order plus time delay processes", *Int. Conf. on System Science and Engineering, ICSSE*, p. 279-283, **2017**.

RERERENCES

[1] Sami, I.; Ullah, S.; Ullah, N.; Ro J.-S. Sensorless fractional order composite sliding mode control design for wind generation system. *ISA Transaction*, 2021, *111*, pp. 275–289.

[2] Correa-Escudero, I.L.; Gómez-Aguilar, J.F.; López- López, M.G.; Alvarado-Martínez, V.M. Correcting dimensional mismatch in fractional models with power, exponential and proportional kernel: Application to electrical systems. *Results in Physics*, 2022, *40*, 105867.

[3] Latif, A.; Hussain, S.M.S.; Das, D.C.; Ustun, T.S.; Iqbal, A. A review on fractional order (FO) controllers' optimization for load frequency stabilization in power network. *Energy Reports*, 2021, *7*, pp. 4009–4021.

[4] Paola, M.D.; Pinnola, F.P. and Zingales, M. Fractional differential equations and related exact mechanical models. *Computers & Mathematics with Applications*, 2013, *66(5)*, pp. 608–620.

[5] Homaeinezhad, M.R.; Shahhosseini, A. Fractional order actuation systems: Theoretical foundation and application in feedback control in mechanical systems. *Applied Mathematical Modelling*, 2020, *87*, pp. 625–639.

[6] Chauchois, A.; Didier, D.; Emmanuel, A.; Bruno, D. Use of noninteger identification models for monitoring soil water content. *Measurement Science and Technology*, 2003, *14(6)*, 868.

[7] Magin, R.L. *Fractional calculus in bioengineering*, Begell House Inc., 2006.

[8] Freeborn, T.J. A survey of fractional-order circuit models for biology and biomedicine, *IEEE Journal on Emerging and Selected Topics in Circuits and Systems*, 2013, *3(3)*, pp. 416–424.

[9] K.S. Miller and B. Ross, *An Introduction to the Fractional Calculus and Fractional Differential Equations*, 1st edtion, Wiley-Interscience, NY, USA, 1993.

[10] Monje, C.A.; Chen, Y.Q.; Vinagre, B.M.; Xue, D.; Feliu, V. *Fractional order Systems and Controls: Fundamentals and Applications*, Springer, London, 2010.

[11] Petrás, I. *Fractional-Order Nonlinear Systems: Modeling, Analysis and Simulation*, Springer Science & Business Media, 2011.

[12] W. Mitkowski, J. Kacprzyk, *Advances in the theory and application of non-integer order systems*, Springer, 2013.

[13] Valério, D.; Costa, J.S.d. *An introduction to fractional control*. The Institution of Engineering and Technology, London, 2013.

[14] Bode, H.W. *Network Analysis and Feedback Amplifier Design*, New York, D. Van Nostrand Company, Inc., 1945

[15] Podlubny, I. Fractional-order systems and $PI^{\lambda}D^{\mu}$ controllers. *IEEE Transactions on Automatic Control*, 1999, *44(1)*, pp. 208–214.

[16] Podlubny, I.; Petrás, I.; Vinagre, B.M.; O'Leary, P.; Dorcák, L. Analogue realizations of fractional-order controllers, *Nonlinear Dynamics*, 2002, *29*, pp. 281–296.

[17] Brancík, L.; Valsa, J.; Gonzalez, E.; Terpak, J.; Petras, I.; Pivka, L. Analogue realizations of fractional-order dynamical systems, *Entropy*, 2013, *15(10)*, pp. 4199–4214.

[18] Li, Z.; Ding, J.; Wu, M.; Lin, J. Discrete fractional order PID controller design for nonlinear systems. *International Journal of Systems Science*, 2021, *52(15)*, pp. 3206–3213.

[19] Malik, S.A.; Mir, A.H. FPGA Realization of Fractional Order Neuron. *Applied Mathematical Modelling*, 2020, *81*, pp. 372–385.

[20] Kapoulea, S.; Psychalinos, C.; Elwakil, A.S.; HosseinNia S. H. Realization of fractional-order PID loop-shaping controller for mechatronic applications. *Integration-the VLSI Journal*, 2021, *80*, pp. 5–12.

[21] Chen, Y.Q.; Petrás, I.; Xue, D. Fractional order control- a tutorial. *Proc. of the American Control Conference (ACC)*, 2009, St. Louis, USA.

[22] Lou, Y. and Chen, Y.Q. Fractional-order [proportional derivative] controller for robust motion control: Tuning procedure and validation. *Proc. of the American Control Conference (ACC)*, 2009, St. Louis, USA.

[23] Monje, C.A.; Calderon, A. J.; Vinagre, B. M.; Feliu, V.; Chen, Y.Q. On fractional PI^{λ} controllers: some tuning rules for robustness to plant uncertainties, *Nonlinear Dynamics*, 2004, *38(1)*, pp. 369–381.

[24] Chen, Y.Q.; Xue, D. and Bhaskaran, T. Practical tuning rule development for fractional order proportional and integral controllers, *Journal of Computational and Nonlinear Dynamics*, 2008, *3(2)*, 021403.

[25] Suárez, I.; Vinagre, B. M.; Calderón, A. J.; Monje, C.A.; Chen, Y.Q. Using fractional calculus for lateral and longitudinal control of autonomous vehicles, A chapter in the Lecture Notes in Computer Science, Springer Verlag, 2003, vol. 2809.

[26] Luo, Y.; Zhang, T.; Lee, B.; Kang, C.; Chen, Y.Q. Disturbance observer design with Bode's ideal cut-off filter in hard-disc-drive servo system mechatronics. *Mechatronics*, 2013, *23(7)*, pp. 856–862.

[27] Luo, Y.; Zhang, T.; Lee, B.; Kang, C.; Chen, Y.Q. Fractional-order proportional derivative controller synthesis and implementation for hard-disk-drive servo system. *IEEE Transactions on Control Systems Technology*, 2014, *22(1)*, pp. 281–289.

[28] Li, Y.; Chen, Y.Q. Stability analysis of fractional order universal adaptive stabilization. *New Trends in Nanotechnology and Fractional Calculus Applications*, 2009, Springer, pp. 357–368.

[29] Jiao, Z.; Chen, Y.Q. Stability of fractional-order linear time-invariant systems with multiple noncommensurate orders. *Computer and Mathematics with Applications*, 2012, *64(10)*, pp. 3053–3058.

[30] Li, Y.; Chen, Y.Q.; Podlubny, I. Mittag-Leffler stability of fractional order nonlinear dynamic systems, *Automatica*, 2009, 45(8), pp. 1965–1969.

[31] Liang, J.; Chen, Y.Q.; Vingre, B. M.; Podlubny, I. Identification of a fractional linear diffusion-wave equation from noisy boundary measurements. *Proc. of the 1st IFAC Symposium on Fractional Differentiation and its Applications*, 2004, Bordeaux, France.

[32] Yin, C.; Dadras, S.; Zhong, S.; Chen, Y.Q. Control of a novel class of fractional-order chaotic systems via adaptive sliding mode control approach. *Applied Mathematical Modelling*, 2013, *37(4)*, pp. 2469–2483.

[33] Malek, H.; Dadras, S.; Chen, Y.Q. A fractional order maximum power point tracker: Stability analysis and experiments. *Proc. of the 51st Annual Conference on Decision and Control (CDC)*, 2012, Maui, Hawaii, USA.

[34] Maamri, N.; Trigeassou, J. C.; Mehdi, D. A frequency approach to the stability of fractional differential equations with time delays. *Proc. of the European Control Conference*, 2009, Budapest, Hungary.

[35] Tenoutit, M.; Maamri, N.; Trigeassou, J.C. An identification procedure for the tuning of a robust fractional controller. *Proc. of the 6th Workshop on Fractional Differentiation and its Applications*, 2013, Grenoble, France.

[36] Malti, R.; Moreau, X.; Khemane, F.; Oustaloup, A. Stability and resonance conditions of elementary fractional transfer functions, *Automatica*, 2011, *47(11)*, pp. 2462–2467.

[37] Malti, R.; Aoun, M.; Sabatier, J.; Oustaloup, A. Tutorial on system identification using fractional differentiation models, *Proc. of the 14th IFAC Symposiumon System Identification*, 2006, Newcastle, Australia.

[38] Malti, R.; Victor, S.; Oustaloup, A. Advances in system identification using fractional models, *Journal of Computational and Nonlinear Dynamics*, 2008, *3(2)*, 021401.

[39] Benchellal, A.; Poinot, T.; Trigeassou, J.C. Fractional modeling and identification of a thermal process. *Journal of Vibration and Control*, 2008, *14(9-10)*.

[40] Victor, S.; Malti, R.; Garnier, H.; Oustaloup, A. Parameter and differentiation order estimation in fractional models. *Automatica*, 2013, *49(4)*, pp. 926–935.

[41] Maachou, A.; Malti, R.; Melchior, P.; Battaglia, J. L; Oustaloup, A; Hay, B. Nonlinear thermal system identification using fractional Volterra series. *Control Engineering Practice*, 2014, 29, pp. 50–60.

[42] Matignon, D. Stability results for fractional differential equations with applications to control processing. *Computational Engineering in Systems and Applications Multiconference*, 1996, *2*, pp. 963–968, Lille, France.

[43] Matignon, D. Stability properties for generalized fractional differential systems. *ESAIM: Proc.*, 1998, *5*, pp. 145–158.

[44] Ahn, H.S.; Chen, Y.Q. Necessary and sufficient stability condition of fractional-order interval linear systems, *Automatica*, 2008, *44(11)*, pp. 2985–2988.

[45] Hamamci, S.E. An algorithm for stabilization of fractional-order time delay systems using fractional-order PID controllers. *IEEE Transactions on Automatic Control*, 2007, 52(10), pp. 1964–1969.

[46] Dzielinski, A.; Sierociuk, D. Stability of discrete fractional oder state-space systems. *Journal of Vibration and Control*, 2008, *14(9-10)*.

[47] Hwanga, C.; Cheng, Y.C. A numerical algorithm for stability testing of fractional delay systems. *Automatica*, 2006, *42(5)*, pp. 825–831.

[48] Hu, W.; Cai, W.J.; Xiao, G. Decentralized Control System Design for MIMO Processes with Integrators/Differntiators. *Ind. Eng. Chem. Res.* 2010, *49(24)*, pp. 12521–12528.

[49] Ammathil, R.; Narsaiah, T.B.; Rao, A.S. Design of decentralised Smith predictor for multivariable non-square processeds with multiple time delays. *Int. J. Modeling, Identification and Control*, 2014, *21(2)*, pp. 147–159.

[50] Chandramohan goud, E.; Rao, A.S.; Chidambaram, M. Improved Decentralized PID Controller design for MIMO processes. *IFAC papersOnline*, 2020, *53(1)*, pp. 153–158.

[51] Wang, Y.J. Tuning optimal and robust decentralized PID controllers for two-input two-ouput time delay systems with a decouper based on frequency domain robustness specifications. *Franklin Open*, 2024, *6*, 100072.

[52] Dan Chen; Seborg, D.E. Relative Gain Array Analysis for Uncertain Process Model. *AIChE Journal*, 2002, 48(2), pp. 302–310.

[53] McAvoy, T.; Arkun, R.; Chen, R.; Robinson, D.; Schnelle, P.D. A New Approach to Defining a Dynamic Relative Gain. *Control Engineering Practice*, 2003, *11(8)*, pp. 907–914.

[54] He, M.J.; Cai, W.J.; Ni, W.; Xie, L.H. RNGA based control system configuration for multivariable processes. *Journal of Process Control*, 2009, *19*, pp. 1036–1042.

[55] Vu, T.N.L.; Lee, M. Independent design of multi-loop PI/PID controllers for interacting multivariable processes. *Journal of Process Control*, 2010, *20*, pp. 922–933.

[56] Kumar, V.V.; Rao, V.S.R.; Chidambaram, M. Centralized PI controllers for interacting multivariable processes by synthesis method. *ISA Transactions*, 2012, *51*, pp. 400–409.

[57] Qin, S.J.; Badgwell, T.A. A survey of industrial model predictive control technology. *Control Engineering Practice*, 2003, *11*, pp. 733–764.

[58] Forbes, M.G.; Patwardhan, R.S.; Hamadah, H.; Gopaluni, R.B. Model Predictive Control in Industry: Challenges and Opportunities. *IFAC PapersOnline*, 2015, *48(8)*, pp.531–538.

[59] Harold L.W. Inverted decoupling: a neglected technique. *ISA Transactions*, 1997, *36(1)*, pp. 3–10.

[60] Gagnon, E.; Pomerleau, A.; Desbiens, A. Simplified, ideal or inverted decoupling? *ISA Transactions*, 1998, *37*, pp. 265–276.

[61] Liu, L.; Tian, S.; Xue, D.; Zhang, T.; Chen, Y.Q.; Zhang, S. A Review of Industrial MIMO Decoupling Control. *International Journal of Control, Automation and Systems*, 2019, *17*, pp. 1–9.

[62] Wang, Q.G.; Huang, B.; Xin, G. Auto-tuning of TITO decoupling controllers from step tests. *ISA Transactions*, 2000, *39*, pp. 407–418.

[63] Chen, P.; Zhang, W. Improvement on an inverted decoupling technique for a class of stable linear multivariable processes. *ISA Transactions*, 2007, *46*, pp.199–210.

[64] Shen, Y.; Cai, W.J.; Li, S. Normalized decoupling control for high-dimensional MIMO processes for application in room temperature control HVAC systems. *Control Engineering Practice*, 2010, *18*, pp. 652–664.

[65] Sun, L.; Dong, J.; Li, D.; Lee, K.Y. A practical multivariable control approach based on inverted decoupling and decentralized active disturbance rejection control. *Ind. Eng. Chem. Res.*, 2016, 55(7), pp. 2008–2019.

[66] Rajapandiyan, C.; Chidambaram, M. Controller Design for MIMO Processes Based on Simple Decoupled Equivalent Transfer Functions and Simplified Decoupler. *Ind. Eng. Chem. Res.*, 2012, *51*, pp. 12398–12410.

[67] Vu, T.N.L.; Lee, M. An Extended Method of Simplified Decoupling for Multivariable Processes with Multiple Time Delays. *Journal of Chem. Eng. Japan*, 2013, *46(4)*, pp. 279–293.
[68] Garrido, J.; Vázquez, F.; Morrila, F. Centralized Inverted Decoupling Control. *Ind. Eng. Chem. Res*., 2013, *52(23)*, pp. 7854–7866.
[69] Garrido, J.; Vázquez, F.; Morilla, F. An extended approach of inverted decoupling. *Journal of Process Control*, 2011, *21(1)*, pp. 55–68.
[70] Garrido, J.; Vázquez, F.; Morilla, F. Inverted decoupling internal model control for square stable multivariable time delay systems. *Journal of Process Control*, 2014, *24(11)*, pp. 1710–1719.
[71] Normey-Rico, J.E.; Camacho, E.F. Unified approach for robust dead-time compensator design, *Journal of Process Control*, 2009, *19(1)*, pp. 38–47.
[72] Sanz, R.; Garcia, P.; Albertos, P. A generalized Smith predictor for unstable time-delay SISO systems. *ISA Transactions*, 2018, *72*, pp. 197–204.
[73] Raja, G.L.; Ali, A. Smith predictor based parallel cascade control strategy for unstable and integrating processes with large time delay. *Journal of Process Control*, 2017, *52*, pp. 57–65.
[74] Torrico, B.C.; Pereira, R.D.O.; Sombra, A.K.R.; Nogueira, F.G. Simplified filtered Smith predictor for high-order dead-time processes, *ISA Transactions*, 2021, *109*, pp. 11–21.
[75] Raja, G.L.; Ali, A. Enhanced tuning of Smith predictor-based series cascaded control structure for integrating processes, *ISA Transactions*, 2021, *114*, pp. 191–205.
[76] Rao, A.S.; Chidambaram, M. Smith delay compensator for multivariable non-square systems with multiple time delays. *Computers and Chem. Eng.*, 2006, *30(8)*, pp. 1243–1255.
[77] Santos, T.L.M.; Torrico, B.C.; Normey-Rico, J.E. Simplified filtered Smith predictor for MIMO processes with multiple time delays. *ISA Transactions*, 2016, *65*, pp. 339–349.
[78] Rodríguez, C.; Normey-Rico, J.E.; Guzmán, J.L.; Berenguel, M. On the filtered Smith predictor with feedforward compensation. *Journal of Process Control*, 2016, *41(1)*, pp. 35–46.
[79] Amaral, D.L.; Torrico, B.C.; Nogueira, F.G.; Pereira, R.D.O.; Santos, T.L.M. A unified tuning rule of the simplified filtered Smith predictor for SISO and square MIMO high-oder dead-time processes. *Control Engineering Practice*. 2023, *141*, 105697.
[80] Garrido, J.; Vázquez, F.; Morilla, F., Normey-Rico, J.E. Smith predictor with inverted decoupling for square multivariable time delay systems. *International Journal of Systems Science*, 2016, *47(2)*, pp. 374–388.
[81] Chen, Y.Q.; Bhaskaran, T.; Xue, D. Practical Tuning Rule Development for Fractional Order Proportional and Integral Controllers. *J. Computational and Nonlinear Dynamics*, 2008, 3(2), 021403.
[82] Li, D.; Liu, L.; Jin, Q.; Hirasawa, K. Maximum sensitivity based fractional IMC-PID controller design for non-integer order system with time delay. *J. Process Control*, 2015, *31*, pp. 17–29.
[83] Amoura K, et al. Closed-loop step response for tuning PID-fractional-order-filter controllers. *ISA Transactions*, 2016, *64*, pp. 247–257.
[84] Li M.; P. Zhou; Z. Zhao; J. Zhang; Two-degree-of-freedom fractional order-PID controllers design for fractional order processes with dead-time. *ISA Transactions*, 2016, *61*, pp. 147-154.
[85] Li, D.; He, X.; Song, T.; Jin, Q. Fractional Order IMC Controller Design for Two-input-two-output Fractional Order System, *International Journal of Control, Automation and Systems*, 2019, *17*, pp. 1–12.
[86] Ranjan, A.; Mehta, U. Fractional filter IMC-TDD controller design for integrating processes. *Results in Control and Optimization*, 2022, *8*, 100155.
[87] Ranjan, A.; Mehta, U.; Saxena, S. A comprehensive review of modified Internal Model Control (IMC) structures and their filters for unstable processes. *Annual Reviews in Control*, 2023, 56, 100895.
[88] Luo, Y.; Chen, Y.Q.; Wang, C.Y.; Pi, Y.G. Tuning fractional order proportional integral controllers for fractional order systems. *J. Process Control*, 2010, *20(7)*, pp. 823–831.

[89] Beschi, M.; Padula, F.; Visioli, A. Fractional robust PID control of a solar furnace. *Control Engineering Practice*, 2016, *56*, pp. 190–199.
[90] Keyser, D.R.; Muresan, C.I.; Ionescu, C.M. A novel auto-tuning method for fractional order PI/PD controllers. *ISA Transactions,* 2016, *62*, pp. 268–275.
[91] Dastjerdi, A.A.; Saikumar, N.; HosseinNia, S.H. Tuning guidlelines for fractional order PID controller: Rules of thumb. *Mechatronics*, 2018, *56*, pp. 26–36.
[92] Dastjerdi, A.A.; Vinagre, B.M.; Chen, Y.Q.; HosseinNia, S.H. Linear fractional order controller: A survey in the frequency domain. *Annual Reviews in Control*, 2019, *47*, pp. 51–70.
[93] Chen, P.; Luo, Y.; Peng, Y.; Chen, Y.Q. Optimal robust fractional order $PI^{\lambda}D$ controller synthesis for first order plus time delay systems. ISA Transactions, 2021, *114*, pp. 136–149.
[94] Yumuk, E.; Guzelkaya, M.; Eksin, I. A robust fractional-order controller design with gain and phase margin specification based on delayed Bode's ideal transfer function. Journal of the Franlink Institute, 2022, *359(11)*, pp. 5341–5353.
[95] Hajiloo, A.; Nariman-zadeh, N.; Moeini, A. Pareto optimal robust design of fractional-order PID controllers for systems with probabilistic uncertainties, *Mechatronics*, 2012, *22*, pp. 788–801.
[96] Moradi, M. A genetic-multivariable fractional order PID control to multi-input multi-output processes, *J. Process Control*, 2014, *24*, pp. 336–343.
[97] Sánchez, H.S.; Padula, F.; Visioli, A. Vilanova, R. Tuning rules for robust FOPID controllers based on multi-objective optimization with FOPDT models. *ISA Transactions*, 2017, *66*, pp. 344–361.
[98] Haji, V.H.; Monje, C.A. Fractional order PID control of a MIMO distillation column process using improved bat algorithm. Soft Computing, 2018, *23(18)*, pp. 8887–8906.
[99] Karahan, O. Design of optimal fractional order fuzzy PID controller based on cuckoo search algorithm for core power control in molten salt reactors. *Progress in Nuclear Energy*, 2021, *139*, 103868.
[100] Roy, P.; Roy, B.K. Fractional order PI control applied to level control in coupled two tank MIMO system with experimental validation, *Control Engineering Practice*, 2016, *48*, pp. 119–135.
[101] Mainardi, F.; Pironi, P. The fractional Langevin equation: Brownian motion revisited. *Extracta Mathematicae*, 1996, *11(1)*, pp. 140–154.
[102] Van der Pol, B.; Van der Mark, J. Frequency demultiplication, *Nature*, 1927, *120(3019)*, pp. 363–364.
[103] Barbosa, R.S.; Machado, J.A.T.; Ferreira, I.M.; Tar, J. K. Dynamics of the fractional-order Van der Pol oscillator. in *Proc. of the IEEE International Conference on Computational Cybernetics (ICCC'04)*, 2004, Vienna, Austria.
[104] Barbosa, R.S.; Vinagre, B.M.; Calderon, A.J. Analysis of the Van der Pol oscillator containing derivatives of fractional order. *Journal of Vibration and Control*, 2007, *13(9–10)*, pp. 1291–1301.
[105] Hristov, J. An exercise with the He's variation iteration method to a fractional Bernoulli equation arising in a transient conduction with a non-linear boundary heat flux", *International Review of Chemical Engineering*, 2012, *4(5)*, pp. 489–497.
[106] Shah, P.; Agashe, S. Review of fractional PID controller. *Mechatronics*, 2016, *38*, pp. 29 – 41.
[107] Das S.; Saha, S.; Gupta, A. On the seclection of tuning methodology of FOPID controllers for the control of higher order processes, *ISA Transactions*, 2011, *50(3)*, pp. 376–388.
[108] Shah, P.; Agashe, S. Design and optimization of fractional PID controller for higher order control system. *International Conference of IEEE* (ICART) 2013, pp. 588–592.
[109] Feliu-Batlle, V.; Rivas-Perez, R.; Castillo-Garcia, F. Fractional order controller robust to time delay variations for water distribution in an irrigation main canal pool. *Computers & Electronics in Agriculture* 2009, *69(2)*, pp. 185–197.
[110] Pan, I.; Das, S.; Gupta, A. Handling packet dropouts and random delays for unstable delayed processes in NCS by optimal tuning of controllers with evolutionary algorithms. *ISA Transactions* 2011, *50(4)*, pp. 557–572.

[111] Cheng, Y.C.; Hwang, C. Stabilization of unstable first-order time delay systems using fractional-order PD controllers. *Journal of Chin. Inst. Eng.* 2006, *29(2)*, pp. 241–249.
[112] Petrás, I. Stability of fractional-order systems with rational orders: A survey *Fractional Calculus and Applied Analysis*, 2009, *10(3)*.
[113] Tavazoei, M.S.; Haeri, M. A note on the stability of fractional order systems. *Math. Comput. Simul.* 2009, *79(5)*, pp. 1566– 576.
[114] Das, S.; Gupta, A. Fractional order modeling of a PHWR under step-back condition and control of its global power with a robust controller. *Nuclear Sci. IEEE Trans*. 2011, *58(5)*, pp.2431–2441.
[115] Manabe, S. Early development of fractional order control. *American society of mechanical engineers*, 2003, pp. 609–619.
[116] Lennart Ljung, *System Identification: Theory for the User*, 2th Edition, Prentice Hall, 1999.
[117] Van den Hof, P.M.J.; Bombois, X. *System Identification for Control*, Lecture Notes DISC Course, March 2004.
[118] Zhu, Y. *Multivariable System Identification for Process Control*, Elsevier Science & Technology Books, 2001.
[119] Liu, T.; Gao, F. *Industrial Process Identification and Control Design*, Springer-Verlag London Limited, 2012.
[120] Hang, C.C.; Astrom, K.J.; Wang, Q.G. Relay feedback auto-tuning of process controllers – a tutorial review. *Journal of Process Control*, 2002, *12*, pp. 143–162.
[121] Zhu, Y. System Identification for Process Control: Recent Experimence and Outlook. *14th IFAC Symposium on System Identification*, Newcastle, Australia, 2006.
[122] Liu, T.; Wang, Q.G.; Huang, H.P. A tutorial review on process identification from step or relay feedback test. *Journal of Process Control*, 2013, *23*, pp. 1597–1623.
[123] De la Torre, L.; Chacón, J.; Sánchez-Moreno, J.; Dormido, S. An event-based adaptation of the relay feedback experiment for frequency response identification of stable processes. *ISA Transactions*, 2023, *139*, pp. 510–523.
[124] Hofreiter, M. Decentralized relay feedback identification of TITO systems. *IFAC PapersOnline*, 2023, *56(2)*, pp. 7759–7764.
[125] Yuz, J.I.; Goodwin, G.C. Robust Identification of Contiuous-time Systems from Sampled Data. in: Garnier, H.; Wang, L. Identification of Continuous-time Models from Sampled Data. *Advances in Industrial Control*. Springer, London, 2008.
[126] Mei, H.; Li, S.; Cai, W.J.; Xiong, Q. Decentralized closed-loop parameter identification for multivariable processes from step responses. *Math. and Computers in Simulation*, 2005, *68*, pp. 171–192.
[127] Bazanella, A.S.; Gevers, M.; Miskovic, L. Closed-Loop Identification of MIMO Systems: A New Look at Identifiability and Experiment Design. *European Journal of Control*, 2010, *3*, pp. 228–239.
[128] Darby, M.L.; Nikolaou, M. Identification test design for multivariable model-based control: an industrial perpective. *Control Eng. Practice*, 2014, *22*, pp. 165–180.
[129] Jin, Q.; Wang, Z.; Wang, J. Least squares based iterative identification for multivariable integrating and unstable processes in closed loop. *Applied Math. and Comp.* 2014, *242*, pp.10–19.
[130] Haggblom, K.E. Improved design of experiments for identification of MIMO systems. *Computer Aided Chemical Engineering*, 2019, *46*, pp. 781–786.
[131] Deniz, F.N.; Tan, N. A Model Identification Method for Tuning of PID Controller in a Smith Predictor Structure. *IFAC-PapersOnline*, 2016, *49(10)*, pp. 13–18.
[132] Burn, K.; Maerte, L.; Cox, C. A Matlab toolbox for teaching modern system identification methods for industrial process control. *Int. Journal of Mechanical Eng. Education*, 2015, *38(4)*.
[133] Malti, R.; Victor, S.; Oustaloup, A.; Garnier, H. An optimal instrumental variable method for continuous-time fractional model identification. in *Proceeding of the 17th IFAC World Congress*, 2008, Seoul, South Korea.
[134] Khadhraoui, A.; Jelassi, K.; Trigeassou, J.C; Melchior, P. Identification of Fractional Model by Least-Squares Method and Instrumental Variable. *Journal of Computational and Nonlinear Dynamics*, 2015, *10*, 050801.

[135] Bouyedda, H.; Ladaci, S.; Sedraoui, M.; Lashab, M.; Identification and Control design for a class of non-minimum Phase dead-time Systems based on fractional-order Smith Predictor and Genetic Algorithm Technique. *Int. J. Dynam. Control*, 2019, *7*, pp. 914–925.

[136] Narang, A. Identification and control of fractional and integer order systems. Ph.D. dissertation, Univeristy of Alberta, Canada, 2012.

[137] Caponetto, R.; Dongola, G.; Fortuna, L.; Petras, I. *Fractional Order Systems: Modelling and Control Applications*, World Scientific, 2010.

[138] Das, S. *Functional Fractional Calculus for System Identification and Controls*, Berlin, Heidelberg: Springer-Verlag, 2008.

[139] S. Skogestad, I. Postlethwaite, *Multivariable Feedback Control: Analysis and Design,* 2nd Edition, John Wiley & Sons, 2001.

[140] Kennedy, J.; Eberhart, R. Particle Swarm Optimization, *Proceedings of the IEEE International Conference on Neural Networks*, 1995, pp. 1942 – 1948.

[141] Guedria, N.B. Improved accelerated PSO algorithm for mechanical engineering optimization problems. *Applied Soft Computing*, 2016, *40*, pp. 455–467.

[142] Wang, D.; Tan, D.; Liu, L. Particle swarm optimization algorithm: an overview. *Soft Computing*, 2018, *22*, pp. 387–408.

[143] Luyben, W.L. Simple method for tuning SISO controllers in multivariable systems. *Ind. Eng. Chem. Process Des. Dev*. 1986, 25, pp. 654–660.

[144] Chuong, V.L.; Vu, T.N.L.; Truong, N.T.N.; Jung, J.H. An Analytical Design of Simplified Decoupling Smith Predictors for Multivariable Processes. *Appl. Sci*. 2019, *9 (12)*, 2487.

[145] Zhang, W. Quantitative Process Control Theory, Taylor & Francis Group, USA, 2012.

[146] Ghosh, S.; Pan, S. Centralized PI controller design method for MIMO processes based on frequency response approximation, *ISA Transactions*, 2021, *110*, pp. 117–128.

[147] Khandelwal, S.; Detroja, K.P., The optimal detuning approach based centralized control design for MIMO processes, *J. of Process Control*, 2020, *96*, pp. 23 – 36.